PHASE PORTRAITS AND BIFURCATION DIAGRAM OF THE GRAY-SCOTT MODEL

TING CHEN[1,2], JAUME LLIBRE[2,*] AND SHIMIN LI[3]

ABSTRACT. We give a complete classification of the phase portraits in the Poincaré disk for the cubic polynomial systems

$$\dot{x} = 1 - x - axy^2, \qquad \dot{y} = -by + axy^2,$$

in $\mathbb{R}^2$ according with the values of its two parameters a and b. These differential systems correspond to the Gray-Scott model. Moreover we provide the bifurcation diagram in the parameter plane (a, b) of these systems.

The Gray-Scott model for studying the autocatalysis has been analyzed by several authors these recent years. The original partial differential equations can be simplified to ordinary differential equations, more precisely to a family cubic polynomial differential systems depending on two parameters a and b. Here we characterize the global dynamics of these cubic systems, taking into account their behavior near the infinity using the Poincaré compactification. Moreover we provide the bifurcation diagram of the phase portraits in the parameter plane (a, b).

1. Introduction and statement of the main results

The Gray-Scott model [13, 18] is a cubic autocatalysis system that exhibits many interesting patterns, see for instance the papers [3, 10, 13, 16, 18] and the references quoted there. This model has been studied with slightly distinct differential equations, here we consider the model given by the differential equations

$$\begin{aligned} \frac{\partial U}{\partial t} &= 1 - U - aUV^2 + D_U \Delta U, \\ \frac{\partial V}{\partial t} &= -bV + aUV^2 + D_V \Delta V, \end{aligned} \tag{1}$$

where $U = U(u, v, t)$ and $V = V(u, v, t)$ are the concentrations of an inhibitor and an activator, $(u, v) \in \mathbb{R}^2$, a and b are positive constants, $D_U > D_V$ are the diffusivities, Δ is the Laplace operator, and t is the time. For more details on the Gray-Scott model see the previous mentioned references.

[0]Corresponding author

2010 *Mathematics Subject Classification.* Primary: 34C07, 34C08.

Key words and phrases. Gray-Scott model, cubic polynomial system, phase portraits, bifurcation diagram, Hopf bifurcation.

In order to obtain information on the dynamics of the partial differential equations (1) some authors have studied the ordinary differential systems

$$\begin{aligned} \dot{x} =& 1 - x - axy^2, \\ \dot{y} =& -by + axy^2, \end{aligned} \tag{2}$$

obtained from systems (1) taking $D_U = D_V \equiv 0$. If we put the keywords "Gray-Scott model" in MathSciNet we obtain 161 references related with this model. As far as we know any of these references studied the complete dynamics of the differential systems (2).

The objective of this paper is to obtain all the phase portraits of the cubic polynomial differential systems (2) for all the values of the parameters $a, b \in \mathbb{R}$ in the Poincaré disk, i.e. including the dynamics of systems (2) at infinity and consequently in its neighborhood. See Section 2 for a summary on the Poincaré compactification.

These recent years many authors have studied the phase portraits of different classes of planar polynomial differential systems, we only quote few of them [2, 4, 5, 12, 6, 7, 8, 9, 14, 15, 17]. From this point of view our paper contributes to study a new class, the class defined by the cubic polynomial differential systems (2).

Assume that a is not zero, otherwise the differential systems (2) become linear. Hence we study the phase portraits of systems (2) and provide their bifurcation diagram in the parameter plane $(a, b) \in \mathbb{R}^2 \setminus \{(0, b) : b \in \mathbb{R}\}$. To do this we will use the Poincaré compactification of the polynomial differential systems. Here we say that two differential systems (2) in the Poincaré disk $\mathbb{D}^2$ are *topologically equivalent* if there exists a homeomorphism $h : \mathbb{D}^2 \to \mathbb{D}^2$ which sends orbits to orbits preserving or reversing the direction of all orbits.

For the polynomial differential systems in the Poincaré disk it is known that the separatrices are all the infinite orbits, all the finite singular points, the separatrices of the hyperbolic sectors of the finite and infinite singular points, and the limit cycles. If Σ denotes the set of all separatrices in the Poincaré disk $\mathbb{D}^2$, Σ is a closed set and the components of $\mathbb{D}^2 \setminus \Sigma$ are called the canonical regions, for more details see [11]. We denote by s, r and LC the number of separatrices, canonical regions and limit cycles, respectively. Our main result is the following theorem.

Theorem 1. *The phase portraits of the planar cubic polynomial differential systems* (2) *are topologically equivalent to the following ones of Figures 1, 2 and 3:*

1.1 *if* $0 < a < f_1(b)$ *and* $b < 0$*;*
1.2 *if* $a = f_1(b)$ *and* $b < 0$*;*
1.3 *if* $a > f_1(b)$ *and* $b < 0$*;*
1.4 *if* $b = 0$ *and* $a > 0$*;*
1.5 *if* $a > f_1(b)$, $a > f_2(b)$ *and* $a > f_5(b)$, *or* $a = f_2(b)$ *and* $b > b_3$*;*
1.6 *if* $a = f_5(b)$ *and* $b_1 < b \le b_3$*;*
1.7 *if* $f_1(b) < a < f_5(b)$, $a > f_4(b)$ *and* $a \ge f_2(b)$*;*
1.8 *if* $a = f_4(b)$ *and* $2 < b \le b_2$*;*
1.9 *if* $a = f_4(b)$ *and* $b_2 < b < b_4$*;*
1.10 *if* $f_2(b) < a < f_4(b)$, *or* $a = f_2(b)$ *and* $4 < b < b_2$*;*
1.11 *if* $f_3(b) < a < f_2(b)$, $a < f_4(b)$ *and* $4 < b < b_2$*;*
1.12 *if* $a = f_3(b)$ *and* $4 < b < b_4$*;*

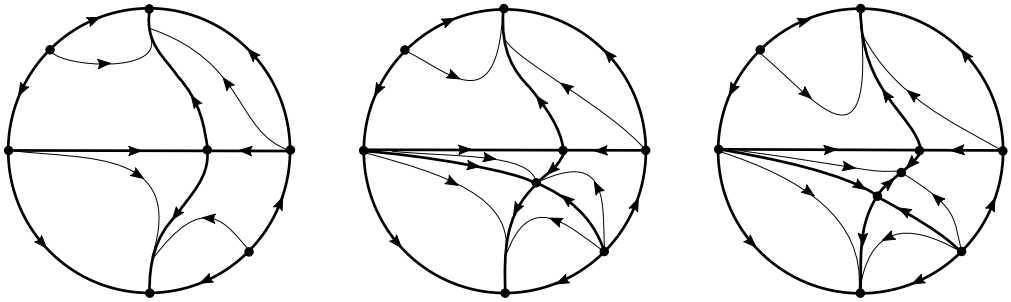

(1.1) s=17, r=4; (1.2) s=21, r=6; (1.3) s=23, r=6;

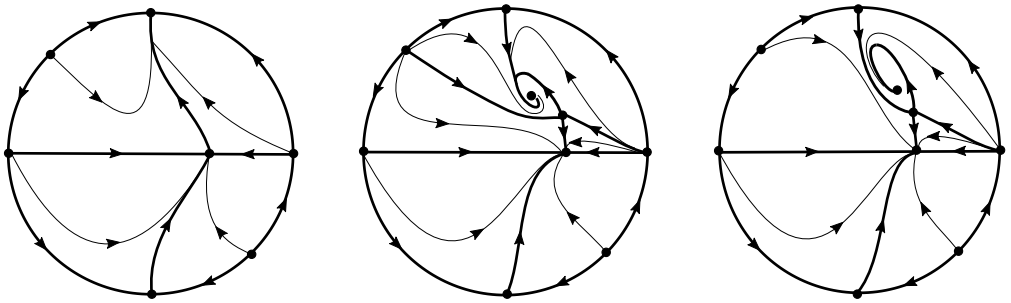

(1.4) s=17, r=4; (1.5) s=23, r=6; (1.6) s=22, r=5;

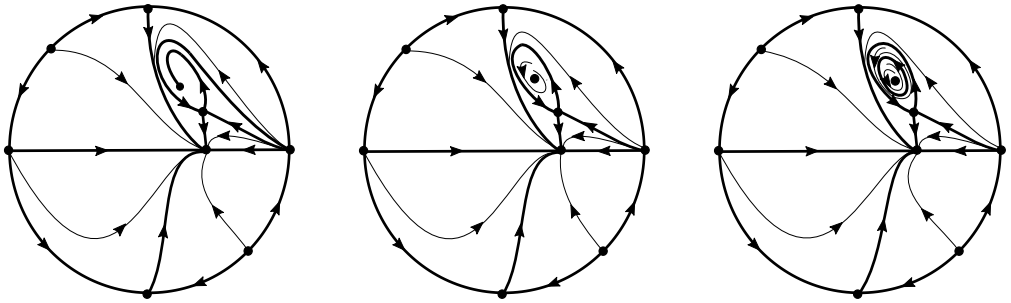

(1.7) s=23, r=6; (1.8) s=22, r=6; (1.9) s=23, r=7, LC=1;

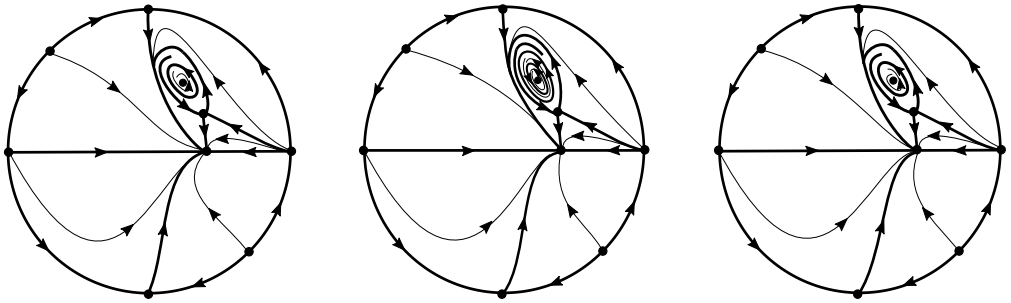

(1.10) s=24, r=7, LC=1; (1.11) s=25, r=8, LC=2; (1.12) s=24, r=7, LC=1.

FIGURE 1. Topological phase portraits of the cases 1.1-1.12 in Theorem 1.

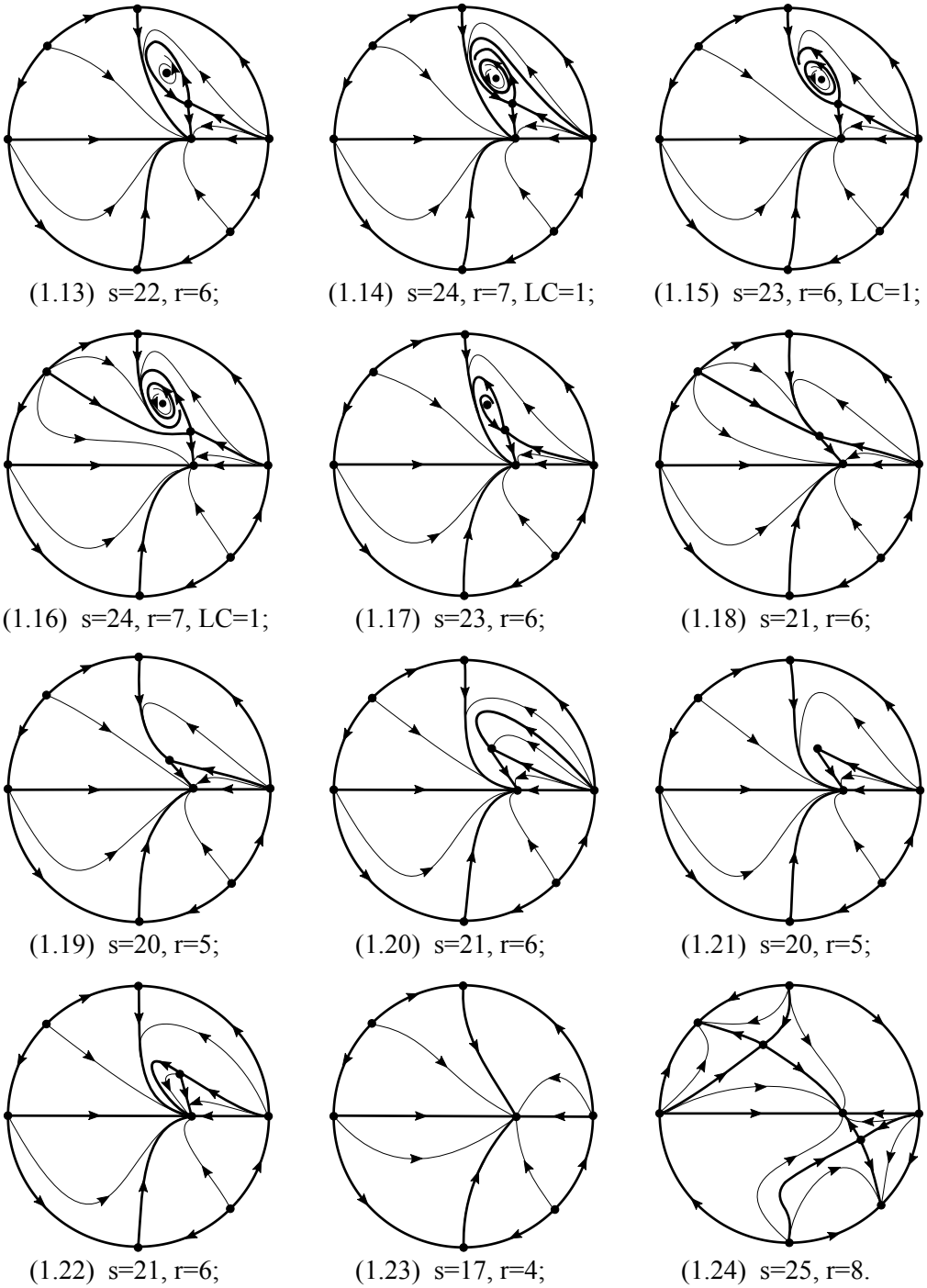

FIGURE 2. Topological phase portraits of the cases 1.13-1.24 in Theorem 1.

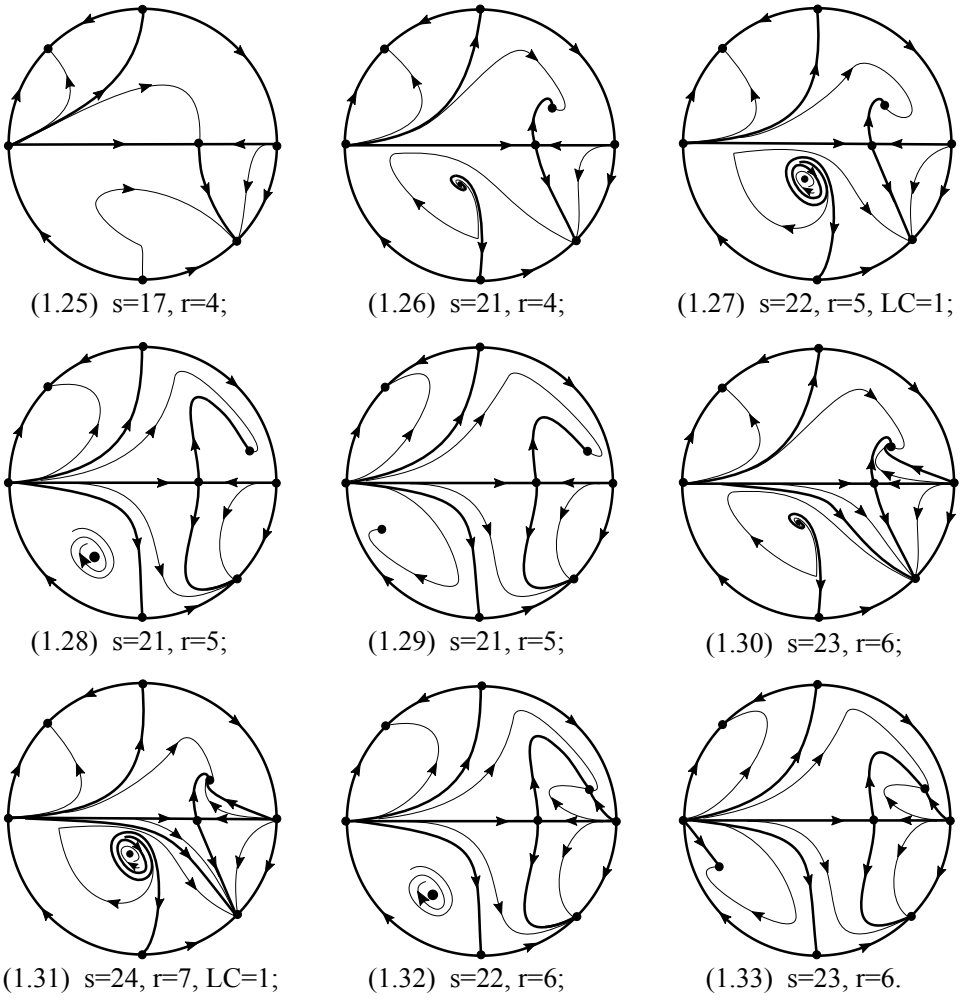

FIGURE 3. Topological phase portraits of the cases 1.25-1.33 in Theorem 1.

1.13 *if* $a = f_4(b)$ *and* $b \geq b_4$*;*
1.14 *if* $f_4(b) < a < f_2(b)$ *and* $a < f_6(b)$*;*
1.15 *if* $a = f_6(b)$ *and* $b > b_3$*;*
1.16 *if* $f_6(b) < a < f_2(b)$ *and* $b > b_3$*;*
1.17 *if* $f_1(b) < a < f_2(b)$, $a < f_3(b)$, $a < f_4(b)$ *and* $b > 2$, *or* $a = f_2(b)$ *and* $2 < b \leq 4$*;*
1.18 *if* $a = f_1(b)$ *and* $0 < b < b_1$*;*
1.19 *if* $a = f_1(b)$ *and* $b = b_1$*;*
1.20 *if* $a = f_1(b)$ *and* $b_1 < b < 2$*;*
1.21 *if* $a = 16$ *and* $b = 2$*;*
1.22 *if* $a = f_1(b)$ *and* $b > 2$*;*
1.23 *if* $0 < a < f_1(b)$ *and* $b > 0$*;*
1.24 *if* $a < 0$ *and* $b > 0$*;*

1.25 *if* $a < 0$ *and* $b = 0$*;*
1.26 *if* $a \leq f_2(b)$ *and* $-1 \leq b < 0$*;*
1.27 *if* $f_2(b) < a < f_7(b)$ *and* $-1 \leq b < 0$*;*
1.28 *if* $a = f_7(b)$ *and* $-1 \leq b < 0$*;*
1.29 *if* $f_7(b) < a < 0$ *and* $-1 \leq b < 0$*;*
1.30 *if* $a \leq f_2(b)$ *and* $b < -1$*;*
1.31 *if* $f_2(b) < a < f_7(b)$ *and* $b < -1$*;*
1.31 *if* $a = f_7(b)$ *and* $b < -1$*;*
1.33 *if* $f_7(b) < a < 0$ *and* $b < -1$*;*

where $f_1(b) = 4b^2$, $f_2(b) = b^4/(b-1)$, $f_i(b)$ $(i = 3, 4, \cdots, 7)$ *are convenient functions,* $b_1 \in (1.4202, 1.4204)$, $b_2 \in (4.4, 4.403)$, $b_3 \in (4.413, 4.414)$ *and* $b_4 \in (6.24, 6.25)$. *Moreover the corresponding bifurcation diagrams are shown in Figures 4, 5 and 6 (see Section 4 for the explanation of the bifurcation diagrams). In fact, the curve* $a = f_1(b)$ *corresponds to a saddle-node bifurcation, the curve* $a = f_2(b)$ *corresponds to a Hopf bifurcation, the curve* $a = f_3(b)$ *corresponds to a semi-stable limit cycle, the curve* $a = f_4(b)$ *corresponds to a homoclinic orbit, the curves* $a = f_5(b)$ *and* $a = f_6(b)$ *correspond to connection of two separatrices, and the curve* $a = f_7(b)$ *corresponds to heteroclinic connection.*

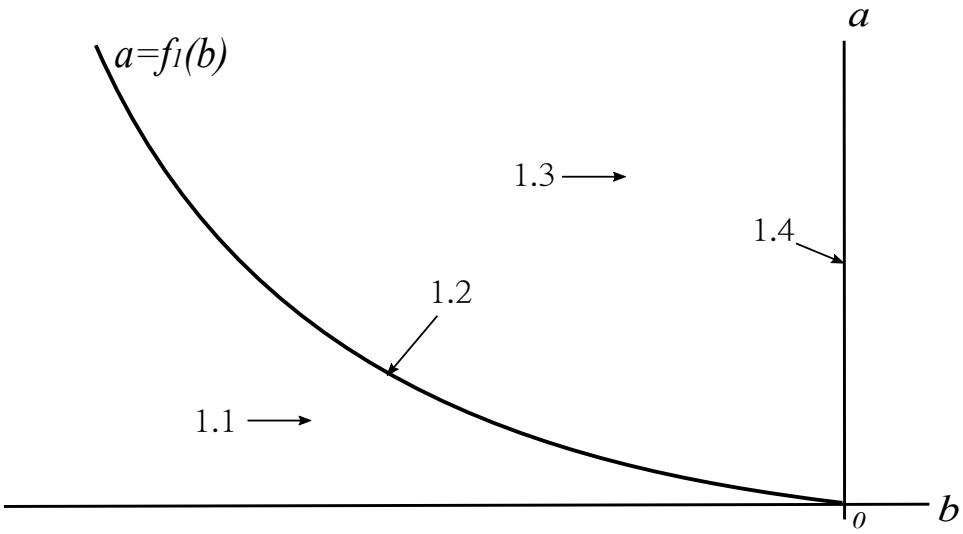

FIGURE 4. The bifurcation diagram of systems (2) when $a > 0$ and $b \leq 0$, where $f_1(b) = 4b^2$.

In this paper we analyze different types of equilibria, hyperbolic, semi-hyperbolic, nilpotent, degenerate and Hopf. For studying the local phase portraits of the semi-hyperbolic equilibria we use Theorem 2.19 of [11], for the nilpotent equilibria we use Theorem 3.5 of [11], while for the degenerate cases we apply blow-ups for studying the local phase portrait at the equilibrium points, for more details on the changes of variables called blow-ups see [1]. And for the Hopf bifurcation we need to compute the Liapunov constants at the singularities. For more information on the Liapunov constants see Chapter 4 of [11]. To complete a global phase portrait of a differential

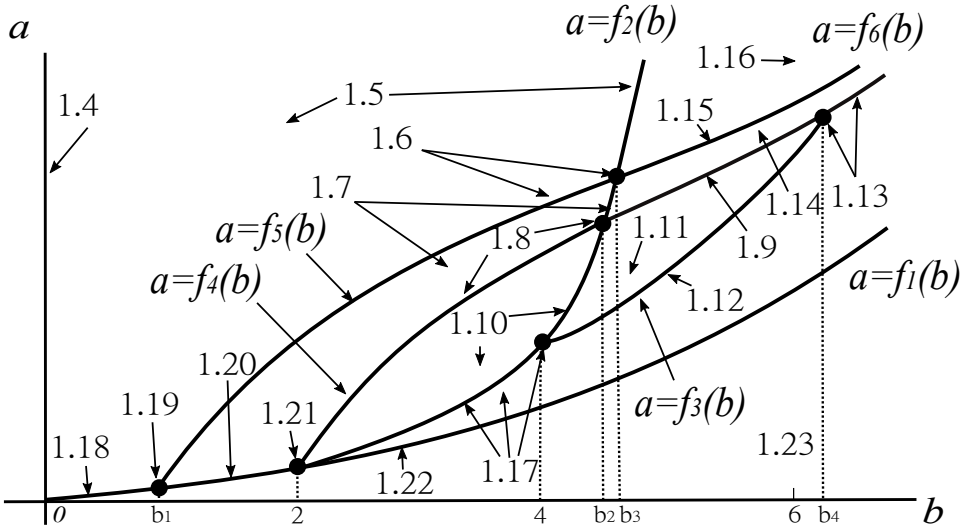

FIGURE 5. The bifurcation diagram of systems (2) when $a > 0$ and $b \geq 0$. $f_1(b) = 4b^2$, $f_2(b) = b^4/(b-1)$, $f_i(b)$ $(i = 3, 4, \cdots, 6)$ are convenient functions, $b_1 \in (1.4202, 1.4204)$, $b_2 \in (4.4, 4.403)$, $b_3 \in (4.413, 4.414)$ and $b_4 \in (6.24, 6.25)$.

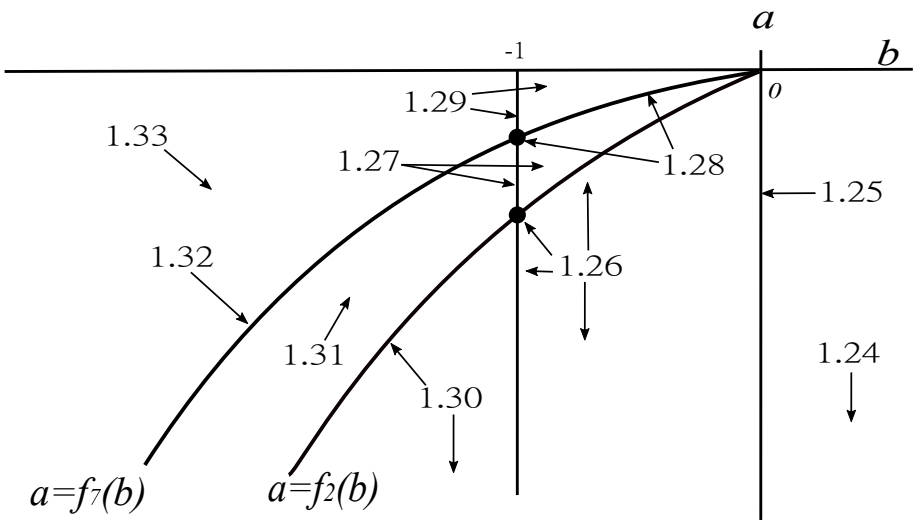

FIGURE 6. The bifurcation diagram of systems (2) when $a < 0$. $f_2(b) = b^4/(b-1)$ and $f_7(b)$ is a convenient function.

system it is important the characterization of its separatrices, and the continuity of phase portraits with respect to the parameters is also essential.

2. Poincaré compactification

In this section we present the Poincaré compactification for describing the phase portraits of the cubic polynomial differential systems (2). See more details in the Chapter 5 of [11].

The sphere $\mathbb{S}^2$ is the set of points $(s_1, s_2, s_3) \in \mathbb{R}^3$ with $s_1^2 + s_2^2 + s_3^2 = 1$, here called the *Poincaré sphere*. Consider a polynomial vector field

$$X = (\dot{x_1}, \dot{x_2}) = (P(x_1, x_2), Q(x_1, x_2)) \tag{3}$$

of degree d in $\mathbb{R}^2$ identified with the plane $x_3 = 1$ of $\mathbb{R}^3$. We can analyze the Poincaré sphere by projecting each point $x \in \mathbb{R}^2$ identified with the point $(x_1, x_2, 1) \in \mathbb{R}^3$ into the Poincaré sphere using a straight line through x and the origin of $\mathbb{R}^3$. Then we obtain a vector field X' formed by two copies of X: one on the northern hemisphere $\{(s_1, s_2, s_3) \in \mathbb{S}^2 : \ s_3 > 0\}$ and another on the southern hemisphere $\{(s_1, s_2, s_3) \in \mathbb{S}^2 : \ s_3 < 0\}$. Note that the equator $\mathbb{S}^1 = \{(s_1, s_2, s_3) \in \mathbb{S}^2 : \ s_3 = 0\}$ corresponds to the infinity of $\mathbb{R}^2$. This vector field X' on $\mathbb{S}^2 \setminus \mathbb{S}^1$ can be extended to a vector field $p(X)$, which is called the *Poincaré compactification* of the vector field X on the whole sphere $\mathbb{S}^2$ multiplying the vector field X' by x_3^d.

What we need for working with the vector field $p(X)$ on the Poincaré sphere are the local charts

$$U_i = \{\mathbf{s} \in \mathbb{S}^2 : \ s_i > 0\}, \ V_i = \{\mathbf{s} \in \mathbb{S}^2 : \ s_i < 0\}, \tag{4}$$

where $\mathbf{s} = (s_1, s_2, s_3)$, with the corresponding local diffeomorphisms

$$\varphi_i(s) : \ U_i \to \mathbb{R}^2, \qquad \psi_i(s) : \ V_i \to \mathbb{R}^2, \tag{5}$$

such the $\varphi_i(s) = -\psi_i(s) = (s_m/s_i, s_n/s_i)$ for $m < n$ and $m, n \neq i$, for $i = 1, 2, 3$. In the local chart U_1 the expression for the corresponding vector field on $\mathbb{S}^2$ is

$$\dot{u} = v^d \Big[-uP\left(\frac{1}{v}, \frac{u}{v}\right) + Q\left(\frac{1}{v}, \frac{u}{v}\right) \Big], \qquad \dot{v} = -v^{d+1} P\left(\frac{1}{v}, \frac{u}{v}\right), \tag{6}$$

the expression in the local chart U_2 is

$$\dot{u} = v^d \Big[-uP\left(\frac{u}{v}, \frac{1}{v}\right) - uQ\left(\frac{u}{v}, \frac{1}{v}\right) \Big], \qquad \dot{v} = -v^{d+1} Q\left(\frac{u}{v}, \frac{1}{v}\right), \tag{7}$$

and the expression in the local chart U_3 is

$$\dot{u} = P(u, v), \qquad \dot{v} = Q(u, v). \tag{8}$$

The expressions for the charts U_i multiplied by $(-1)^{d-1}$, provide the expression for the charts V_i, for $i = 1, 2, 3$.

To study the vector field X it is enough to study its Poincaré compactification $p(X)$ restricted to the northern hemisphere plus $\mathbb{S}^1$. To draw the phase portraits we will consider the orthogonal projection $\pi(s_1, s_2, s_3) = (s_1, s_2)$ of the closed northern hemisphere onto the closed unit disc centered at the origin of coordinates in the plane $x_3 = 0$. This closed disc $\mathbb{D}^2$ is the Poincaré disk.

Using U_3, finite singular points of X, which are the singular points of its compactification in $\mathbb{S}^2 \setminus \mathbb{S}^1$. Infinite singular points of X are the singular points of the corresponding vector field in the Poincaré disk lying on $\mathbb{S}^1$. If $\mathbf{s} \in \mathbb{S}^1$ is an infinite

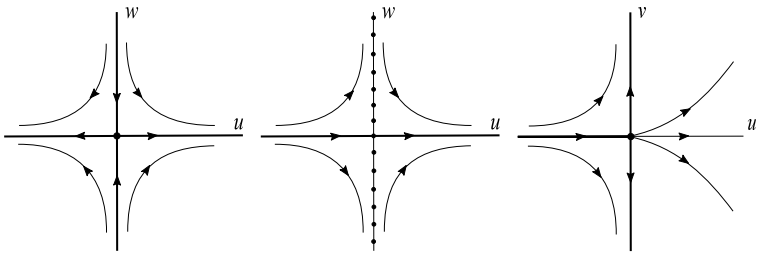

(a) Systems (11) (b) Systems (10) (c) Systems (9)

FIGURE 7. Blow-up of the origin of U_1 when $a > 0$.

singular point, then $-\mathbf{s} \in \mathbb{S}^1$ is another infinite singular point, and the local behavior of one is that of the other multiplied by $(-1)^{d-1}$. Note that for studying the infinite singular points it suffices to look the ones at $U_1|_{v=0}$ and at the origin of U_2. We note that the coordinates (u, v) means different things in every local charts, but in the local charts U_i and V_i for $i = 1, 2$ the infinite points have always the coordinate $v = 0$.

We note that the local phase portraits of a node and a focus are topological equivalent.

3. Phase portraits of systems (2)

We remark that the straight line $y = 0$ of systems (2) is invariant by the flow of these systems. That is, it is formed by orbits of systems (2). This simplifies the study of the phase portraits of systems (2).

3.1. **The infinite singular points.** For the study of the infinite singular points of systems (2) we use the Poincaré compactification, and we first restrict our attention to the local chart U_1. In this chart systems (2) become

$$\begin{aligned} \dot{u} =& u(au + au^2 + v^2 - bv^2 - v^3), \\ \dot{v} =& v(au^2 + v^2 - v^3). \end{aligned} \tag{9}$$

On the infinity, i.e. on $v = 0$, there are two singular points on U_1, namely $A' = (0, 0)$ and $B' = (-1, 0)$. The linear part of systems (9) is

$$\begin{pmatrix} au(2 + 3u) & 0 \\ 0 & au^2 \end{pmatrix}.$$

Hence the singular point B' is an attracting node or a repelling node when $a < 0$ or $a > 0$, respectively.

At the origin A' of U_1 the linear part is identically zero. We need to do blow-up's in order to determine its the local phase portrait. Doing the blow-up $(u, v) \mapsto (u, w)$ with $w = v/u$ we obtain the systems

$$\begin{aligned} \dot{u} =& u^2(a + au + uw^2 - buw^2 - u^2w^3), \\ \dot{w} =& uw(-a + buw^2). \end{aligned} \tag{10}$$

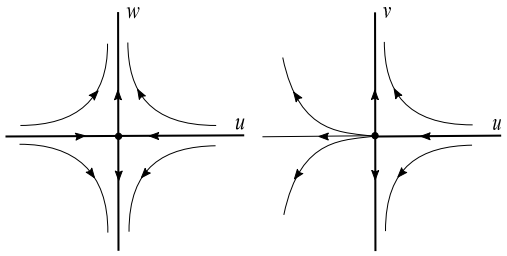

(a) Systems (11) (b) Systems (9)

FIGURE 8. Blow-up of the origin of U_1 when $a < 0$.

Doing a rescaling of the time we eliminate the common factor u between $\dot{u}$ and $\dot{w}$, and we get the systems

$$\begin{aligned} \dot{u} =& u(a + au + uw^2 - buw^2 - u^2w^3), \\ \dot{w} =& w(-a + buw^2). \end{aligned} \tag{11}$$

When $u = 0$ the unique singular point of systems (11) is the origin. The eigenvalues of the linear part of systems (11) at the origin are $\pm a$, hence the origin is a saddle. Going back through the changes of variables until systems (9), we find that A' is a saddle-node point as it is shown in Figures 7 and 8, that is a singular point whose neighborhood consists of one parabolic sector and two hyperbolic sectors.

Now we check if the origin of the local chart U_2 is a singular point. In U_2 we use (7) to get

$$\begin{aligned} \dot{u} =& -au - au^2 + (b-1)uv^2 + v^3 = -au + B(u,v), \\ \dot{v} =& -v(au - bv^2) = A(u,v). \end{aligned} \tag{12}$$

The origin C' of systems (12) is a singular point, and it is a semi-hyperbolic singular point. Assume $a < 0$ then we get that

$$u = f(v) = \frac{v^3}{a} + O(v^5) \tag{13}$$

is the solution of the equation $-au + B(u,v) = 0$ in a neighborhood of the origin. Substituting the variable u from (13) into $A(u,v)$, we have

$$g(v) = A(f(v), v) = bv^3 - v^4 + O(v^5).$$

From Theorem 2.19 of [11], we obtain that there always exists an invariant analytic curve, called the strong unstable manifold, tangent at 0 to the u-axis, on which the vector field is analytically conjugate to

$$\dot{u} = -au,$$

it represents repelling behavior if $a < 0$. Moreover, if $b < 0$ then C' is a saddle, see Figure 9(a). If $b > 0$ it is a repelling node, see Figure 9(b). If $b = 0$ it is a saddle-node, see Figure 9(c).

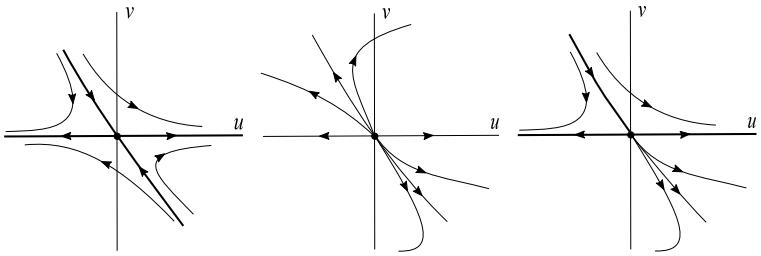

(a) $b < 0$ (b) $b > 0$ (c) $b = 0$

FIGURE 9. The origin of systems (12) when $a < 0$.

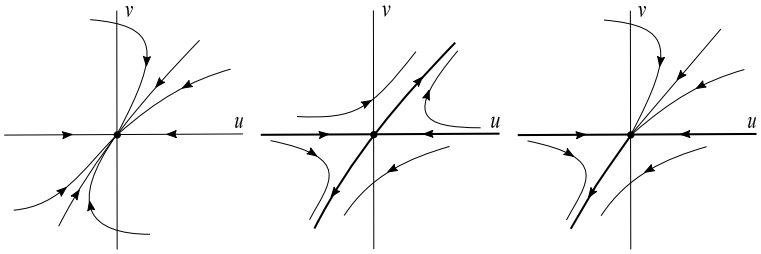

(a) $b < 0$ (b) $b > 0$ (c) $b = 0$

FIGURE 10. The origin of systems (12) when $a > 0$.

Similar to the case $a < 0$, if $a > 0$ by changing the sign of the time $t \mapsto -t$, systems (12) become

$$\begin{aligned} \dot{u} =& au + au^2 + (1-b)uv^2 - v^3 = au + \widetilde{B}(u,v), \\ \dot{v} =& v(au - bv^2) = \widetilde{A}(u,v). \end{aligned} \tag{14}$$

Then we choose the solution $u = f(v) = v^3/a + O(v^5)$ of the equation $au + \widetilde{B}(u,v) = 0$ in a neighborhood of the origin. Substituting the variable u into $\widetilde{A}(u,v)$, we obtain

$$g(v) = \widetilde{A}(f(v),v) = -bv^3 + v^4 + O(v^5).$$

Due to the change $t \mapsto -t$, we know that the trajectories of systems (12) are traveled in the converse direction to the ones of systems (14). Hence we have that C' is an attracting node when $b < 0$ (see Figure 10(a)), a saddle when $b > 0$ (see Figure 10(b)), and a saddle-node when $b = 0$ (see Figure 10(c)).

For systems (2) we have found six equilibria in the infinite region, two (A' and B') are in U_1, one (C') is in U_2 and their diametrically opposite (A'', B'' and C'') are in V_1 and V_2. Note that for systems (2) the degree is 3 so the flow in the charts V_1 and V_2 have the same sense than in the charts U_1 and in U_2, respectively.

3.2. **The finite singular points.** Having determined the local phase portraits at the infinite singular points of systems (2), we now compute the phase portraits at their finite singular points. We separate the study of the finite singular points

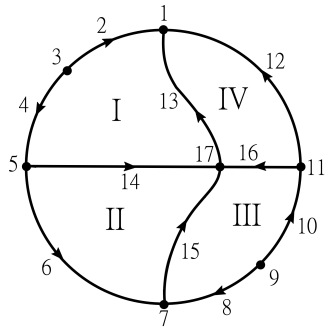

FIGURE 11. The number of separatrices and of canonical regions of systems (2) when $a > 0$ and $b = 0$.

in three cases: (i) either $a(a - 4b^2) < 0$ or $b = 0$, (ii) $a = 4b^2 \neq 0$, and (iii) $a(a - 4b^2) > 0$ and $b \neq 0$.

Case (i). If either $a(a - 4b^2) < 0$ or $b = 0$, that is either $0 < a < 4b^2$, or $b = 0$. Then systems (2) have the unique finite singular point $(1, 0)$.

Subcase (i.a). Assuming $b = 0$ the linear part of systems (2) is

$$M = \begin{pmatrix} -1 - ay^2 & -2axy \\ ay^2 & 2axy \end{pmatrix}. \tag{15}$$

Thus $(1, 0)$ is a semi-hyperbolic singular point of systems (2). We move it to the origin doing the translation $x \mapsto x + 1$, and in order to apply Theorem 2.19 of [11] we reverse the sign of the time $t \mapsto -t$, and we get the systems

$$\begin{aligned} \dot{x} =& x + a(x + 1)y^2 = x + D(x, y), \\ \dot{y} =& -a(x + 1)y^2 = C(x, y). \end{aligned} \tag{16}$$

Then

$$x = f(y) = -ay^2 + O(y^3)$$

is the solution of the equation $x + D(x, y) = 0$ in a neighborhood of the origin of systems (16). Therefore we have

$$g(y) = C(f(y), y) = ay^2 + O(y^3).$$

From Theorem 2.19 of [11] we obtain that the singular point $(1, 0)$ of systems (2) (or the origin of systems (16)) is a saddle-node.

In this case taking into account the local phase portraits at the infinite and finite singular points together with the fact that the straight line $y = 0$ is invariant systems (2) have 17 separatrices and 4 canonical regions in their phase portraits when $a > 0$, see Figure 11. Then we obtain the phase portraits 1.4 of Figure 1 and 1.25 of Figure 3 for $a > 0$ and $a < 0$, respectively.

Subcase (i.b). If $0 < a < 4b^2$ since the linear part of systems (2) is given in (15), we get that $(1, 0)$ is a saddle when $b < 0$. Therefore the phase portrait of systems (2) is topologically equivalent to the phase portrait 1.1 of Figure 1. When $b > 0$ the singular point $(1, 0)$ is an attracting node. Therefore the only possible phase portrait in this case is the 1.23 of Figure 2.

Case (ii). If $a = 4b^2 \neq 0$ systems (2) have two finite singular points $(1,0)$ and $(1/2, 1/(2b))$. As in the subcase (i.b) we have that $(1,0)$ is an attracting node or a saddle when $b > 0$ or $b < 0$, respectively. Now we study the local phase portrait of the singular point $(1/2, 1/(2b))$. The eigenvalues of (15) at $(1/2, 1/(2b))$ are 0 and $-2 + b$.

Subcase (ii.a) If $b = 2$ the singular point $(1/2, 1/4)$ is a nilpotent singular point. We translate this singular point to the origin doing the change of variables $x \mapsto x+1/2$, $y \mapsto y + 1/4$, and we have the systems

$$\begin{aligned} \dot{x} =& -2(x + 2y + 4xy + 4y^2 + 8xy^2) = H(x,y), \\ \dot{y} =& (1 + 4y)(x + 2y + 4xy) = x + G(x,y). \end{aligned} \tag{17}$$

Therefore

$$x = f(y) = -2y + O(y^2)$$

is the solution of the equation $x + G(x,y) = 0$ in a neighborhood of the origin of systems (17). Then we obtain

$$H(y) = H(f(y), y) = -8y^2 + O(y^3)$$

and

$$\left(\frac{\partial G}{\partial y} + \frac{\partial H}{\partial x}\right)(f(y), y) = -8y + O(y^2).$$

From Theorem 3.5 of [11] we obtain that the singular point $(1/2, 1/4)$ of systems (2) (or the origin of systems (17)) is a cusp. Hence in this subcase we have the phase portrait 1.21 of Figure 2.

Subcase (ii.b) Assuming $b \neq 2$ the point $(1/2, 1/(2b))$ is a semi-hyperbolic singular point. We move the point $(1/2, 1/(2b))$ to the origin doing the translation $x \mapsto x + 1/2$, $y \mapsto y + 1/(2b)$, and in order to apply Theorem 2.19 of [11] we reverse the sign of the time $t \mapsto -t$, and we obtain the systems

$$\begin{aligned} \dot{x} =& 2(x + by + 2bxy + b^2y^2 + 2b^2xy^2) = 2x + F(x,y), \\ \dot{y} =& -(1 + 2by)(x + by + 2bxy) = E(x,y), \end{aligned} \tag{18}$$

Then

$$x = f(y) = -by + O(y^2)$$

is the solution of the equation $2x + F(x,y) = 0$ in a neighborhood of the origin of systems (18). Hence we have

$$g(y) = E(f(y), y) = b^2y^2 + O(y^3).$$

From Theorem 2.19 of [11] it follows that the singular point $(1/2, 1/(2b))$ of systems (2) (or the origin of systems (18)) is a saddle-node. In summary we obtain the phase portrait 1.2 of Figure 1 when $b < 0$, the phase portrait 1.18 of Figure 2 when $0 < b < b_1$, the phase portrait 1.20 of Figure 2 when $b_1 < b < 2$, and the phase portrait 1.22 of Figure 2 when $b > 2$. By the continuity of the phase portraits moving the parameter b we obtain the phase portrait 1.19 when $(a,b) = (4b_1^2, b_1)$, in this phase portrait two separatrices have connected. It is difficult to get the value of b_1, but b_1 belongs to the interval (1.4202,1.4204).

Case: (iii). If $a(a-4b^2)>0$, then either $a>4b^2$ or $a<0$, additionally we can assume $b\neq 0$. The finite singular points of systems (2) different from $(1,0)$ are

$$p_1=(x_1,y_1)=\left(\frac{1}{2}+\frac{\sqrt{a(a-4b^2)}}{2a},\frac{a-\sqrt{a(a-4b^2)}}{2ab}\right),$$
$$p_2=(x_2,y_2)=\left(\frac{1}{2}-\frac{\sqrt{a(a-4b^2)}}{2a},\frac{a+\sqrt{a(a-4b^2)}}{2ab}\right).$$

Similarly to the above case we get that $(1,0)$ is an attracting node or a saddle when $b>0$ or $b<0$, respectively. Next we consider two subcases and some subsubcases in order to study the local phase portraits of the singular points p_1 and p_2.

Subcase (iii.a). Assuming $a>4b^2$ we have that the determinant and the trace of (15) at p_1 are

$$\text{Det}[M]\Big|_{p_1}=\frac{a-4b^2-\sqrt{a(a-4b^2)}}{2b},\ \text{Tr}[M]\Big|_{p_1}=\frac{-a+2b^3+\sqrt{a(a-4b^2)}}{2b^2}. \tag{19}$$

Similarly we obtain

$$\text{Det}[M]\Big|_{p_2}=\frac{a-4b^2+\sqrt{a(a-4b^2)}}{2b},\ \text{Tr}[M]\Big|_{p_2}=\frac{-a+2b^3-\sqrt{a(a-4b^2)}}{2b^2}. \tag{20}$$

Now we shall study the local phase portraits at the singular points p_1 and p_2. For this we need to know the sign of $\text{Tr}[M]|_{p_1}$ or $\text{Tr}[M]|_{p_2}$. Hence we give the Remarks 2 and 3.

Remark 2. *From* $\text{Tr}[M]|_{p_1}<0$ *we have either* $b<0$ *and* $b^4/(b-1)<a\leq 0$, *or* $b<0$ *and* $a\geq 4b^2$, *or* $0<b\leq 1$ *and* $a\geq 4b^2$, *or* $1<b<2$ *and* $4b^2\leq a<b^4/(b-1)$. *From* $\text{Tr}[M]|_{p_1}=0$ *we have* $a=b^4/(b-1)$ *and* $a\geq 2b^3$. *From* $\text{Tr}[M]|_{p_1}>0$ *we have either* $b\leq 0$ *and* $a<b^4/(b-1)$, *or* $b>0$ *and* $a\leq 0$, *or* $1<b\leq 2$ *and* $a>b^4/(b-1)$, *or* $b>2$ *and* $a\geq 4b^2$.

Remark 3. *From* $\text{Tr}[M]|_{p_2}<0$ *we have either* $b<0$ *and* $a\leq 0$, *or* $b<0$ *and* $a\geq 4b^2$, *or* $0<b<1$ *and* $a<b^4/(b-1)$, *or* $0<b<2$ *and* $a\geq 4b^2$, *or* $b\geq 2$ *and* $a>b^4/(b-1)$. *From* $\text{Tr}[M]|_{p_2}=0$ *we have* $a=b^4/(b-1)$ *and* $a\leq 2b^3$. *From* $\text{Tr}[M]|_{p_2}>0$ *we have either* $0<b<1$ *and* $b^4/(b-1)<a\leq 0$, *or* $1\leq b$ *and* $a\leq 0$, *or* $b>2$ *and* $4b^2\leq a<b^4/(b-1)$.

Subsubcase (iii.a.1). If $b>0$ we have $1>x_1>x_2>0$ and $y_2>y_1>0$. On the other hand, we get $\text{Det}[M]|_{p_1}<0$, because

$$(a-4b^2)^2-a(a-4b^2)=4b^2(4b^2-a)<0.$$

Hence the singular point p_1 is a saddle. From (20) we obtain that $\text{Det}[M]|_{p_2}$ is positive. Then we need to compute the discriminant

$$\Delta_1=\left[(\text{Tr}[M])^2-4\text{Det}[M]\right]\Big|_{p_2}=\frac{N_1}{2b^4} \tag{21}$$

where

$$N_1=a^2-2ab^2-6ab^3+16b^5+2b^6+(a-6b^3)\sqrt{a(a-4b^2)}. \tag{22}$$

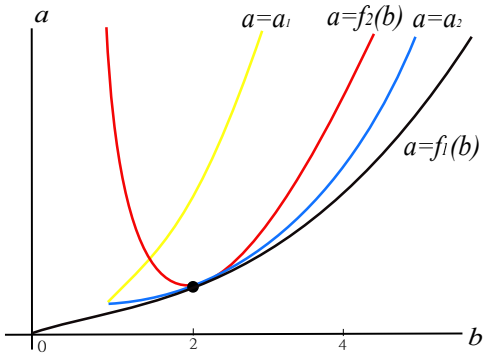

FIGURE 12. The roots $a_{1,2}$ of N_1 when $a > 0$. $f_1(b) = 4b^2$, $f_2(b) = b^4/(b-1)$.

When $0 < b < 1$ it is easy to check that $N_1 > 0$, because it has no real roots. In addition we have $\mathrm{Tr}[M]|_{p_2} < 0$, hence the singular point p_2 is an attracting node, and we get the phase portrait 1.5 of Figure 1.

If $b \geq 1$ the equation $N_1 = 0$ has two roots

$$a_{1,2} = \frac{b^3(8+7b+3b^2) \pm 2\sqrt{2(-1+b)b^7(2+b)^2}}{1+2b+b^2}. \tag{23}$$

The graphics of $a_{1,2}$, which help us to analyze the singular points $p_{1,2}$, see Figure 12. Since

$$b^6(8+7b+3b^2)^2 - 8(-1+b)b^7(2+b)^2 = b^6(1+b)^2(8+b)^2 > 0,$$

it is easy to get that $0 < 4b^2 \leq a_2 \leq a_1$. Then we have $N_1 \geq 0$ when $4b^2 < a \leq a_2$ or $a \geq a_1$.

We have $\mathrm{Tr}[M]|_{p_2} < 0$ when $a \geq a_1$, or $1 \leq b < 2$ and $4b^2 < a \leq a_2$. Hence the singular point p_2 is an attracting node. In this subsubcase the phase portraits are topologically equivalent to 1.5-1.7 of Figure 1. From the phase portraits 1.5 and 1.7 it follows by the continuity of the phase portraits with respect to the parameters the existence of the phase portrait 1.6. Hence we obtain the bifurcation curve $a = f_5(b)$ on which we have the phase portrait 1.6. Note that the intersection of the curves $a = f_5(b)$ and $a = f_1(b)$ is the point $(4b_1^2, b_1)$.

We have $\mathrm{Tr}[M]|_{p_2} > 0$ when $b > 2$ and $4b^2 < a \leq a_2$. Hence the singular point p_2 is a repelling node. In this case the phase portraits of systems (2) are topologically equivalent to 1.17 of Figure 2.

On the other hand, we have $N_1 < 0$ when $a_2 < a < a_1$. Thus the singular point p_2 is a stable focus when $\mathrm{Tr}[M]|_{p_2} < 0$, that is $1 < b < 2$, $a_2 < a < a_1$ and $a \neq b^4/(b-1)$, or $b > 2$ and $b^4/(b-1) < a < a_1$. The phase portraits are topologically equivalent to 1.5-1.7 of Figure 1. The singular point p_2 is an unstable focus when $\mathrm{Tr}[M]|_{p_2} > 0$, that is $2 < b$ and $a_2 < a < b^4/(b-1)$. The phase portrait is topologically equivalent to 1.17 of Figure 2.

When $a = b^4/(b-1)$ and $b \neq 2$ we have either $\mathrm{Tr}[M]|_{p_1} = 0$, or $\mathrm{Tr}[M]|_{p_2} = 0$. Indeed, if from Remarks 2 and 3 we have $\mathrm{Tr}[M]|_{p_1} = \mathrm{Tr}[M]|_{p_2} = 0$ if and only if

$(a,b)=(0,0)$ or $(a,b)=(16,2)$, which is in contradiction with $a>4b^2$. Simplifying $a_2<b^4/(b-1)<a_1$, we have $-1+\sqrt{5}<b<2$ or $2<b$.

Assume that $a=b^4/(b-1)$ and $2<b$, we have the singular points $p_1'=((b-1)/b,1/b^2)$ and $p_2'=(1/b,(b-1)/b^2)$ where $1>(b-1)/b>1/b>0$ and $(b-1)/b^2>1/b^2$. From $\mathrm{Tr}[M]|_{p_2'}=0$ and $\Delta_1=-4(b-2)b<0$, we get that p_2' must be a center or a focus. We move p_2' to the origin doing the translation $x\mapsto x+1/b$, $y\mapsto y+(b-1)/b^2$, and we get the systems

$$\begin{aligned}\dot{x}=&-bx-2by-2b^2xy-\frac{b^3}{b-1}y^2-\frac{b^4}{b-1}xy^2,\\ \dot{y}=&(b-1)x+by+2b^2xy+\frac{b^3}{b-1}y^2+\frac{b^4}{b-1}xy^2.\end{aligned}\tag{24}$$

Doing the change of variable $(x,y,t)\mapsto(\xi,\eta,\tau)$ where

$$\begin{aligned}\xi=&\frac{b-\sqrt{(b-2)b}i}{4b}x+\frac{b+\sqrt{(b-2)b}i}{4b}y,\\ \eta=&\frac{\sqrt{(b-2)b}-3bi}{4b}x-\frac{\sqrt{(b-2)b}+3bi}{4b}y,\\ \tau=&\sqrt{(b-2)b}t,\ i=\sqrt{-1},\end{aligned}$$

systems (24) become

$$\begin{aligned}\frac{d\xi}{d\tau}=&-\eta-\frac{(3b-4)\sqrt{(b-2)b}}{2(b-2)(b-1)}\xi^2-\frac{(b-2)b}{b-1}\xi\eta+\frac{b\sqrt{(b-2)b}}{2(b-1)}\eta^2\\ &+\frac{b^3\sqrt{(b-2)b}}{(b-2)(b-1)}\xi^3+\frac{2b^3}{b-1}\xi^2\eta+\frac{b^2\sqrt{(b-2)b}}{b-1}\xi\eta^2,\\ \frac{d\eta}{d\tau}=&\xi-\frac{b^2(3b-4)}{2(b-2)(b-1)}\xi^2-\frac{b\sqrt{(b-2)b}}{b-1}\xi\eta+\frac{b^2}{2(b-1)}\eta^2\\ &\frac{b^4}{(b-2)(b-1)}\xi^3+\frac{2b^3\sqrt{(b-2)b}}{(b-2)(b-1)}\xi^2\eta+\frac{b^3}{b-1}\xi\eta^2.\end{aligned}\tag{25}$$

We present some basic formulas for computing the Liapunov constants of the general differential systems

$$\begin{aligned}\dot{x}=&\delta x-\beta y+\sum_{k=2}^{n}P_k(x,y),\\ \dot{y}=&\beta x+\delta y+\sum_{k=2}^{n}Q_k(x,y),\end{aligned}\tag{26}$$

where $P_k(x,y)$, $Q_k(x,y)$ are homogeneous polynomials of degree k in x and y. Introducing the polar coordinate transformation, $x=\rho\cos\theta$ and $y=\rho\sin\theta$, system (26) can be written as the differential equation

$$\frac{\mathrm{d}\rho}{\mathrm{d}\theta}=\frac{\delta\rho+\sum_{k=2}^{n}\Upsilon_k(\theta)\rho^k}{\beta+\sum_{k=2}^{n}\Theta_k(\theta)\rho^{k-1}},\tag{27}$$

where

$$\begin{aligned}\Upsilon_k(\theta)=&\cos\theta P_k(\cos\theta,\sin\theta)+\sin\theta Q_k(\cos\theta,\sin\theta),\\ \Theta_k(\theta)=&\cos\theta Q_k(\cos\theta,\sin\theta)-\sin\theta P_k(\cos\theta,\sin\theta),\end{aligned}$$

in which P_k and Q_k are polynomials in $\sin\theta$ and $\cos\theta$. The general solution of (27) in a neighborhood of the origin can be expressed as

$$\Pi(\rho,\theta)=\sum_{k\geq 1} v_k(\theta)\rho^k, \quad |\rho|\ll 1, \tag{28}$$

and we define the displacement function

$$d(\rho)=\Pi(\rho,2\pi)-\rho=(v_1-1)\rho+\sum_{k\geq 1} v_{2k+1}\rho^{2k+1}, \tag{29}$$

where v_k ($v_{2k}\equiv 0$) is called the kth-order Liapunov constant at the origin of systems (26). The number of fixed points of $d(\rho)$ (or zeros of $d(\rho)$) corresponds to the number of limit cycles of systems (29). If the displacement function (29) satisfies $v_1=1$, $v_3=\cdots=v_{2k-1}=0$ and $v_{2k+1}\neq 0$, any perturbation of (26) have at most k limit cycles bifurcating at the origin.

Then we compute the first and the third Liapunov constants of systems (25) at the origin and we obtain $v_1=1$ and

$$v_3=\frac{(4-b)b^2\sqrt{(b-2)b}\pi}{2(b-2)^2}. \tag{30}$$

If $v_3=0$, namely $b=4$, the fifth Liapunov constant is

$$v_5=\frac{b^4\sqrt{(b-2)b}(192-1228b+1417b^2-567b^3+72b^4)\pi}{12(b-2)^4(b-1)}=\frac{256\sqrt{2}\pi}{3}>0.$$

So the origin of systems (25) is an unstable weak focus of second order. The phase portrait is topologically equivalent to 1.16 of Figure 2. From [19, Theorem 2] and since the derivative

$$\left.\frac{\partial v_3}{\partial b}\right|_{b=4}=4\sqrt{2}\pi\neq 0,$$

then there exist exactly two small amplitude limit cycles bifurcating from the singular point p_2' of systems (2) (or from the origin of systems (24)) by small perturbation of $b=4$, see Figure 13. We obtain the phase portrait 1.11 of Figure 1. In order to obtain two small amplitude limit cycles, it requires to find a set of explicit perturbation value b, which is not an easy task. We give the convenient function $f_3(b)$ to describe the region, whose existence is given by continuity for proving from the phase portrait 1.11 to 1.17. When $a=f_3(b)$, systems (2) have only one semi-stable (externally unstable and internally stable) limit cycle. Hence, the phase portrait is topologically equivalent to 1.12 of Figure 1.

If $2<b<4$ the third Liapunov constant $v_3>0$ from (30), we have that the singular point p_2' is an unstable weak focus. Furthermore we obtain a phase portrait which is topologically equivalent to the phase portrait 1.17 of Figure 2. There exists exactly one small amplitude limit cycle bifurcating from the singular point p_2' of systems (2) by small perturbation of b. In fact, in the neighborhood of the curve $a=b^4/(b-1)$ the singularity p_2' is an unstable focus when $a<b^4/(b-1)$ and a stable focus when $b^4/(b-1)<a$. The stability of the focus reverses, and a Hopf bifurcation occurs, there must bifurcate one limit cycle from this singular point. Hence we obtain the phase portrait 1.10 of Figure 1. There exists a convenient function $f_4(b)$, its existence is given by continuity between the phase portraits 1.7 to 1.10, i.e. at the curve $a=f_4(b)$ systems (2) have a homoclinic loop, and

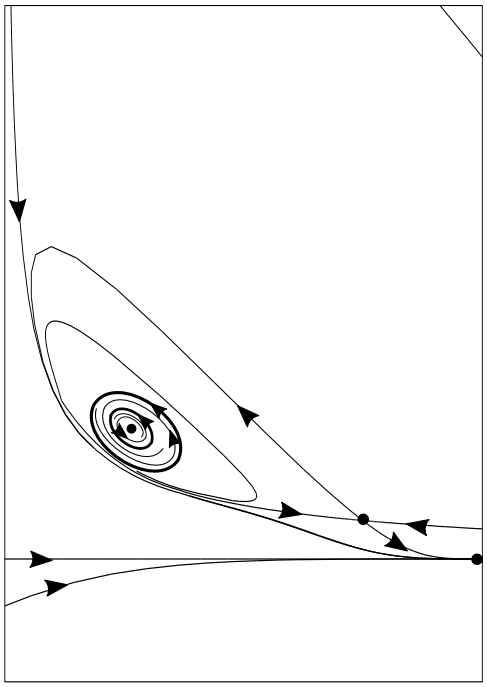

FIGURE 13. Two small amplitude limit cycles bifurcated from the singular point p_2' of systems (2).

topologically their phase portrait is the 1.8 of Figure 1. We get that the coordinate of the point corresponding to the intersection point of the curves $a = f_2(b)$ and $a = f_4(b)$ is $(b_2^4/(b_2-1), b_2)$, and b_2 belongs to $(4.4, 4.403)$.

Similarly, if $b > 4$ the singular point p_2' is a stable weak focus. The phase portraits are topologically equivalent to 1.5-1.7 of Figure 1. And there exists exactly one small amplitude limit cycle bifurcating from the singular point p_2' of systems (2). Hence we obtain the phase portraits 1.10 of Figure 1 and 1.14-1.16 of Figure 2. From the phase portraits 1.14 and 1.16, we obtain the bifurcation curve $a = f_6(b)$ which corresponds to the phase portrait 1.15. In addition, it is difficult to obtain the coordinates of the intersection point (a, b_3) between the curves $a = f_5(b)$ and $a = f_6(b)$. But we can get that $b_3 \in (4.413, 4.414)$.

Now we assume $a = b^4/(b-1)$ and $\sqrt{5}-1 < b < 2$, and we have that the singular points $p_1' = (1/b, (b-1)/b^2)$ and $p_2' = ((b-1)/b, 1/b^2)$ where $1 > 1/b > (b-1)/b > 0$ and $1/b^2 > (b-1)/b^2$. The trace of M at p_2' is $\mathrm{Tr}[M]|_{p_2'} = (b-2)b/(b-1) < 0$ and the discriminant is $b(8-8b+b^3) < 0$. Hence the singular point p_2' is a stable focus. Then the phase portraits are topologically equivalent to 1.5-1.7 of Figure 1.

By the continuity of the phase portraits with respect to parameters from the phase portrait 1.11 to 1.14, we obtain the bifurcation curve $a = f_4(b)$ with $b_2 < b < b_4$ which describes the phase portrait 1.9, i.e. systems (2) have a homoclinic loop with a limit cycle inside the loop. The intersection point of the curves $a = f_3(b)$ and $a = f_4(b)$ is $(f_4(b_4), b_4)$, and b_4 belongs to the interval $(6.24, 6.25)$. On the

other hand, from the phase portrait 1.14 to 1.17 we obtain the phase portrait 1.13, i.e. systems (2) have a homoclinic loop in the bifurcation curve $a = f_4(b)$ with $b \geq b_4$.

Subsubcase (iii.a.2). If $b < 0$ we have $1 > x_1 > x_2 > 0$ and $y_2 < y_1 < 0$. From (20) we have $\mathrm{Det}[M]|_{p_2} < 0$. Therefore the singular point p_2 is a saddle. Since $\mathrm{Det}[M]|_{p_1} > 0$ from (19) we obtain that the discriminant at p_1 is

$$\Delta_2 = \Big[(\mathrm{Tr}[M])^2 - 4\mathrm{Det}[M]\Big]\Big|_{p_1} = \frac{N_2}{2b^4},$$

where

$$N_2 = a^2 - 2ab^2 - 6ab^3 + 16b^5 + 2b^6 + (6b^3 - a)\sqrt{a(a-4b^2)}. \tag{31}$$

When $b = -1$ we obtain

$$N_2 = a^2 + 4a - 14 - \sqrt{a^3(a-4)} - 6\sqrt{a(a-4)} > 0.$$

If $b \neq -1$ solving $N_2 = 0$ for a we obtain the same solutions $a_{1,2}$ given in (23), see Figure 14. We have

$$\lim_{b\to -1} a_1 = -\frac{49}{8} \text{ and } \lim_{b\to -1} a_2 = -\infty.$$

It is easy to check that $a_2 \leq a_1 \leq 0$ when $b < 0$. Hence we have $N_2 \geq 0$ and

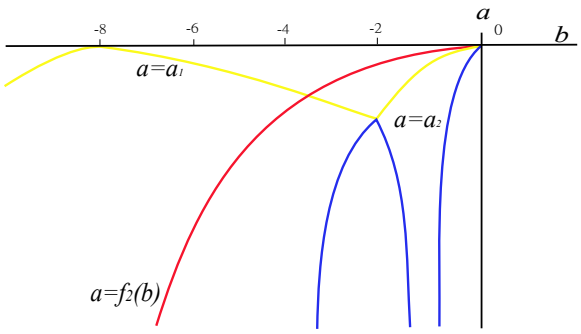

FIGURE 14. The roots $a_{1,2}$ of $N_2 = 0$ when $a < 0$. $f_2(b) = b^4/(b-1)$.

$\mathrm{Tr}[M]|_{p_1} < 0$, because $a > 4b^2$. Furthermore we get that the singular point p_1 is an attracting node. The only possible phase portrait in this case is 1.3 of Figure 1.

Subcase (iii.b). Assume $a < 0$.

Subsubcase (iii.b.1). If $b > 0$ we have $x_1 < 0$, $x_2 > 1$, $y_1 > 1/b$ and $y_2 < 0$. Consequently $\mathrm{Det}[M]|_{p_1} < 0$ and $\mathrm{Det}[M]|_{p_2} < 0$, because

$$(a - 4b^2)^2 - a(a - 4b^2) = 4b^2(4b^2 - a) > 0. \tag{32}$$

Hence the singular points $p_{1,2}$ are saddles, and we obtain the phase portrait 1.24 of Figure 2.

Subsubcase (iii.b.2). If $b < 0$ we have $x_1 < 0$, $x_2 > 1$, $y_1 < 1/b$ and $y_2 > 0$. From (32) it is easy to check that $\mathrm{Det}[M]|_{p_1} > 0$ and $\mathrm{Det}[M]|_{p_2} > 0$. And we have $\mathrm{Tr}[M]|_{p_2} < 0$ from Remark 3. Hence the singular point p_2 must be stable. From

(22) and (31) we need to determine the signs of N_i for $i = 1, 2$ for characterizing the local phase portraits at the singular points p_1 and p_2.

Assume $b = -1$.

We obtain that $N_1 = 0$ has no solution, and N_2 has one solution $a = -49/8$.

1) If $a = -1/2$ we have $N_1 < 0$ and $N_2 < 0$. So the singular point $p_2' = (2, 1)$ is a stable focus. On the other hand, we have $\mathrm{Tr}[M]|_{p_1'} = 0$. Then the singular point $p_1' = (-1, -2)$ is a center or a focus. From (30) we have that the third Liapunov constant of p_1' is

$$v_3 = \frac{5\sqrt{3}\pi}{18} > 0.$$

Thus the singular point p_1' is an unstable weak focus. Then the phase portrait is 1.26 of Figure 3. Furthermore the Liapunov constant is independent of b, hence there exists exactly one small amplitude limit cycle bifurcating from p_1' of systems (2) under small perturbations. The phase portrait is topologically equivalent to 1.27 of Figure 3.

2) If $0 > a > -49/8$ and $a \neq -1/2$, we get $N_1 < 0$ and $N_2 < 0$. Hence the singular point p_2 is a stable focus. By Remark 2 the trace of M at p_1' is positive or negative when $-49/8 < a < -1/2$ or $-1/2 < a < 0$, respectively. Then p_1 is an unstable focus or a stable focus. Hence we obtain the phase portraits 1.26 of Figure 3 or 1.29 of Figure 3. By the continuity of the phase portraits, we give the point $(f_7(-1), -1)$ to describe one case, whose existence is given by continuity going from the phase portraits 1.27 to 1.29, systems (2) have a heteroclinic orbit. Then the phase portrait in this case turn out to be topologically equivalent to 1.28 of Figure 3.

3) If $a \leq -49/8$ we obtain $N_1 < 0$ and $N_2 > 0$. We have $\mathrm{Tr}[M]|_{p_1} > 0$ from Remark 2. So the singular points p_1 and p_2 are a repelling node and a stable focus, respectively. The node has the same topology with the focus. Therefore the phase portrait is topologically equivalent to 1.26 of Figure 3.

Assume $b \neq -1$.

For determining the signs of N_i for $i = 1, 2$, we solve $N_i = 0$ for a, and we obtain the same solutions $a_2 \leq a_1$, see (23). On the other hand, from $N_1 = 0$ we have

$$a^2 - 2ab^2 - 6ab^3 + 16b^5 + 2b^6 = (6b^3 - a)\sqrt{a(a - 4b^2)}. \tag{33}$$

Thus we obtain

$$\Delta' = (a^2 - 2ab^2 - 6ab^3 + 16b^5 + 2b^6)(6b^3 - a) \geq 0, \tag{34}$$

when $N_1 = 0$. Taking $a = a_1$ into the above inequality, we get $-8 \leq b \leq -2$. If $b = -8$ we have $a = a_1 = 0$, which is not possible because $a < 0$. If $a = a_2$ then, from inequality (34) we get $-2 \leq b < -1$ or $-1 < b < 0$.

Similarly, we have $\Delta' \leq 0$ when $N_2 = 0$. Taking $a = a_1$ into this inequality $\Delta' \leq 0$, we have $b < -8$ or $-2 \leq b < -1$. If $a = a_2$ we obtain $b \leq -2$ from $\Delta' \leq 0$. Hence we have Table 1. Now we analyze the local phase portraits of the singular points p_1 and p_2 by the sign of N_2 and N_1, respectively.

Assume $-1 < b < 0$.

TABLE 1. The solutions of $N_1 = 0$ and $N_2 = 0$ when $b < 0$.

The value of b	The solutions of $N_1 = 0$	The solutions of $N_2 = 0$
$b \in (-1, 0)$	$a = a_2$	$a = a_1$
$b = -1$	no solution	$a = -\frac{49}{8}$
$b \in (-2, -1)$	$a = a_2$	$a = a_1$
$b = -2$	$a = -48$	$a = -48$
$b \in (-8, -2)$	$a = a_1$	$a = a_2$
$b = -8$	$a = 0$	$a = 0$ or $a = -\frac{147456}{49}$
$b \in (-\infty, -8)$	no solution	$a = a_{1,2}$

We get that $N_1 = 0$ has one solution $a = a_2$, and $N_2 = 0$ has one solution $a = a_1$ from Table 1.

1) If $a_1 < a < 0$ and $a = b^4/(b-1)$, we get $N_1 < 0$ and $N_2 < 0$. Hence we have that $p_2' = ((b-1)/b, 1/b^2)$ is a stable focus. The trace of M at $p_1' = (1/b, (b-1)/b^2)$ is $\mathrm{Tr}[M]|_{p_1'} = 0$. From (30) we have the third Liapunov constant $0 < v_3$ at p_1'. Hence the singular point p_1' is an unstable weak focus. Therefore we obtain that the phase portrait is topologically equivalent to 1.26 of Figure 3. Furthermore the Liapunov constant is independent of b, hence there exists exactly one small amplitude limit cycle bifurcating from p_1' of systems (2) under small perturbations. The phase portrait is topologically equivalent to 1.27 of Figure 3.

2) If $a_1 < a < 0$ and $a \neq b^4/(b-1)$, we have $N_1 < 0$ and $N_2 < 0$. Hence the singular point p_2 is a stable focus. From Remark 2 we get that $\mathrm{Tr}[M]|_{p_1} > 0$ when $a_1 < a < b^4/(b-1)$, and $\mathrm{Tr}[M]|_{p_1} < 0$ when $b^4/(b-1) < a < 0$. Hence the singular point p_1 is an unstable focus or a stable focus. The phase portrait is topologically equivalent to 1.26 of Figure 3 or 1.29 of Figure 3. By continuity from the phase portraits 1.27 to 1.28, we obtain the curve $a = f_7(b)$ where systems (2) have a heteroclinic loop. Then the phase portrait in this case turn out to be topologically equivalent to 1.28 of Figure 3.

3) If $a_2 < a \leq a_1$ we have $N_1 < 0$ and $N_2 \geq 0$. So p_2 is a stable focus. From Remark 2 we have $\mathrm{Tr}[M]|_{p_1} > 0$. Hence the singular points p_1 is a repelling node. The phase portrait is topologically equivalent to 1.26 of Figure 3.

4) If $a \leq a_2$ we have $N_1 \geq 0$ and $N_2 > 0$. So we obtain that p_2 is an attracting node. We have $\mathrm{Tr}[M]|_{p_1} > 0$ from Remark 2. Hence the singular points p_1 is a repelling node. Consequently the phase portrait is topologically equivalent to 1.26 of Figure 3.

Assume $-8 < b < -1$.

From Table 1, we get that $N_1 = 0$ and $N_2 = 0$ has one solution, respectively.

1) If $a_1 < a < 0$ and $a = b^4/(b-1)$, we have $N_1 < 0$ and $N_2 < 0$. Hence the singular point $p_2' = ((b-1)/b, 1/b^2)$ is a stable focus. The trace of M at $p_1' = (1/b, (b-1)/b^2)$ is $\mathrm{Tr}[M]|_{p_1'} = 0$. Furthermore from (30) we get that the singular points p_1' is an unstable weak focus. The phase portrait is topologically equivalent to 1.30 of Figure 3. Furthermore the Liapunov constant is independent of b, hence systems (2) have

exactly one small amplitude limit cycle bifurcating from p_1' under small pertubation. In this case the only possible phase portrait is topologically equivalent to 1.31 of Figure 3.

2) If $a_1 < a < 0$ and $a \neq b^4/(b-1)$, we have $N_1 < 0$ and $N_2 < 0$. Then the singular point p_2 is a stable focus. And from Remark 2 we have $\mathrm{Tr}[M]|_{p_1} > 0$ or $\mathrm{Tr}[M]|_{p_1} < 0$ when $a_1 < a < b^4/(b-1)$ or $b^4/(b-1) < a < 0$, respectively. So the singular point p_1 is an unstable focus or a stable focus. Therefore the phase portraits are equivalent to 1.30 or 1.33 of Figure 3. When $a = f_7(b)$ systems (2) have a heteroclinic loop. In this case the phase portrait is topologically equivalent to 1.32 of Figure 3.

3) If $a_2 < a \leq a_1$ and $a = b^4/(b-1)$, we obtain $N_1 \geq 0$ and $N_2 < 0$. From Remark 2 we get that $\mathrm{Tr}[M]|_{p_1'} = 0$. It is easy check that p_1' is an unstable weak focus and p_2' is an attracting node. Consequently we obtain the phase portrait 1.30 of Figure 3. Furthermore the Liapunov constant is independent of b, hence there exists exactly one small amplitude limit cycle bifurcating from p_1' of systems (2). We obtain that the phase portrait is topologically equivalent to 1.31 of Figure 3.

4) If $-2 \leq b < -1$ and $a_2 < a \leq a_1$, we have $N_1 < 0$ and $N_2 \geq 0$. So p_2 is a stable focus. From Remark 2 we have $\mathrm{Tr}[M]|_{p_1} > 0$. Hence the singular point p_1 is a repelling node. If $b < -2$, $a_2 < a < b^4/(b-1)$ and $a < a_1$, we have $N_1 > 0$ and $N_2 < 0$. We have $\mathrm{Tr}[M]|_{p_1} > 0$ from Remark 2. Therefore p_1 is an unstable focus and p_2 is an attracting node. Then we easily get that the phase portraits are topologically equivalent to 1.30 of Figure 3.

5) If $b^4/(b-1) < a < a_1$ we get that $N_1 > 0$ and $N_2 < 0$. It is easy to check that $\mathrm{Tr}[M]|_{p_1} < 0$. So p_1 is a stable focus and p_2 is an attracting node. Therefore the phase portrait is topologically equivalent to 1.32 or 1.33 shown in Figure 3.

6) If $a \leq a_2$ we get $N_1 > 0$ and $N_2 \geq 0$. From Remark 2, we obtain $\mathrm{Tr}[M]|_{p_1} > 0$. Hence p_1 and p_2 are a repelling node and an attracting node. The phase portrait is topologically equivalent to 1.30 of Figure 3.

Remark 4. *Assume $b < 0$. If $a_1 \leq b^4/(b-1)$ then $-1-\sqrt{5} \leq b < -1$ or $-1 < b < 0$. If $a_2 < b^4/(b-1) < a_1$ then $b < -1-\sqrt{5}$. On the other hand, there is no parameter b satisfying $b^4/(b-1) \leq a_2$.*

Assume that $b \leq -8$.

If $b < -8$ we obtain that $N_1 = 0$ has no solution, and $N_2 = 0$ has two solutions $a = a_{1,2}$. If $b = -8$, $N_1 = 0$ has no solution, and $N_2 = 0$ has one solution.

1) If $a_1 \leq a < 0$ we have $N_1 > 0$ and $N_2 \geq 0$. On the other hand, from Remark 4 we have $b^4/(b-1) < a < 0$. Then we have $\mathrm{Tr}[M]|_{p_1} < 0$ from Remark 2. Hence p_1 and p_2 are two attracting nodes. The phase portrait is topologically equivalent to 1.33 of Figure 3.

2) If $a_2 < a < a_1$ and $a = b^4/(b-1)$ (let $a_1 = 0$ and $a_2 = -147456/49$ when $b = -8$), we get that $N_1 \geq 0$ and $N_2 < 0$. Hence $p_2' = ((b-1)/b, 1/b^2)$ is an attracting node. The trace of M at $p_1' = (1/b, (b-1)/b^2)$ is $\mathrm{Tr}[M]|_{p_1'} = 0$. Furthermore from (30) we obtain that p_1' is an unstable weak focus. It is easy to see that the phase portrait is topologically equivalent to the phase portrait 1.30 of Figure 3. Furthermore

the Liapunov constant is independent of b, hence there exists exactly one small amplitude limit cycle bifurcating from p_1' of systems (2). We obtain that the phase portrait is topologically equivalent to 1.31 of Figure 3.

3) If $a_2 < a < b^4/(b-1)$ we obtain $N_1 > 0$ and $N_2 < 0$. It is easy to get that $\mathrm{Tr}[M]|_{p_1} > 0$. Then p_1 is an unstable focus and p_2 is an attracting node. The phase portrait is topologically equivalent to 1.30 of Figure 3.

4) If $b^4/(b-1) < a < a_1$ we get that $N_1 > 0$ and $N_2 < 0$. From Remark 2 we have $\mathrm{Tr}[M]|_{p_1} < 0$. Thus p_1 is a stable focus and p_2 is an attracting node. The phase portrait is topologically equivalent to the phase portrait 1.33 of Figure 3. When $a = f_7(b)$ systems (2) have a heteroclinic loop. The phase portrait is topologically equivalent to 1.32 of Figure 3.

5) If $a \le a_2$ we get $N_1 > 0$ and $N_2 \ge 0$. Then p_2 is an attracting node. On the other hand, we have $\mathrm{Tr}[M]|_{p_1} > 0$ from Remark 2. Hence p_1 is a repelling node. Thus the phase portraits in this case turn out to be topologically equivalent to 1.30 of Figure 3.

This completes the classification of the phase portraits of systems (2) in the parameter plane $(a, b) \in \mathbb{R}^2 \setminus \{(0, b) : b \in \mathbb{R}\}$. From systems (2), if $a = 0$ we obtain linear systems

$$\dot{x} = 1 - x, \qquad \dot{y} = -by. \tag{35}$$

If $b \neq 0$ systems (35) have one finite singular point $(1, 0)$. It is an unstable node when $b > 0$, or a saddle when $b < 0$. If $b = 0$ systems (35) have the straight line $x = 1$ filled of singular points. Then we give the bifurcation diagram of the finite singular points, see Figure 15. Here, we denote by S, N, SN and AS the saddle, the node, the saddle-node and the anti-saddle, i.e. a node or focus.

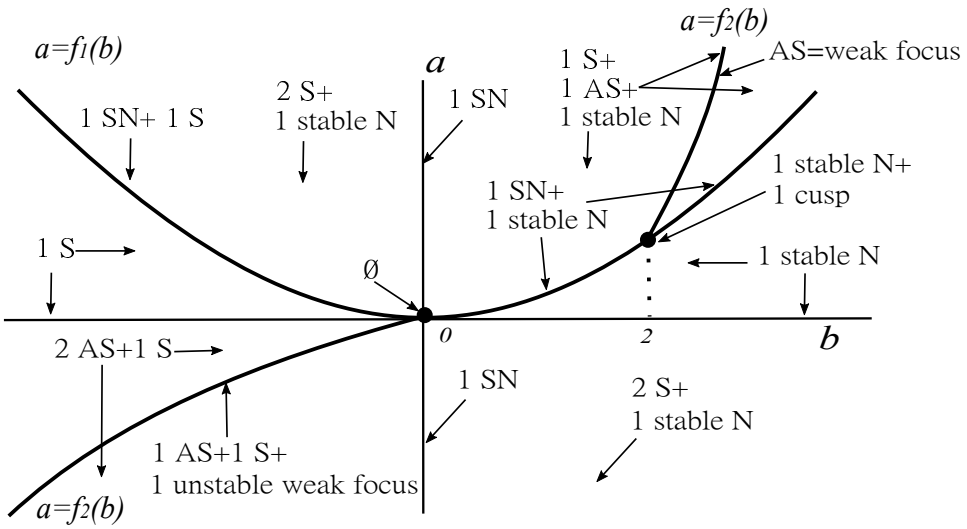

FIGURE 15. The bifurcation diagram of finite singular points of systems (2) where $f_1(b) = 4b^2$, $f_2(b) = b^4/(b-1)$.

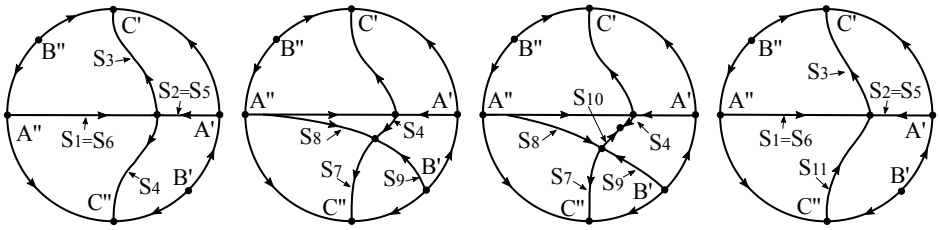

FIGURE 16. Some separatrices of the phase portraits. (a) phase portrait 1.1, (b) phase portrait 1.2, (c) phase portrait 1.3, (d) phase portrait 1.4.

4. Bifurcation diagrams

Now we explain the bifurcation diagrams of the phase portraits of systems (2) in the parameter plane $(a, b) \in \mathbb{R}^2 \setminus \{(0, b) : b \in \mathbb{R}\}$. We note that the bifurcation lines for the phase portraits are $b = 0$ and $a = f_i(b)$ $(i = 1, \cdots, 7)$. The bifurcation diagrams are described in Figures 4, 5 and 6. From the following analysis it would be at most 20 different separatrices, which are not at infinity, connecting with the infinite, finite equilibrium points or with the limit cycle and the homoclinic loop, see Table 2.

TABLE 2. The separatrices, which are not at infinity, connecting the infinite, the finite equilibrium points, or with the limit cycle and the homoclinic loop.

Equilibria	Type of the equilibria	Separatrices
$(1, 0)$	saddle or saddle-node	S_1, S_2, S_3,S_4
p_1	saddle, saddle-node, cusp or focus	S_{13}, S_{14}, S_{15}, S_{16}, L_3
p_2	saddle, saddle-node or focus	S_7, S_8, S_9, S_{10}, H_1, L_1, L_2
A'	saddle-node	S_5
A''	saddle-node	S_6
C'	saddle or saddle-node	S_{12}
C''	saddle or saddle-node	S_{11}

When the parameter (a, b) in Figure 4 provides the phase portrait 1.1, see Figure 16(a), systems (2) have six infinite equilibria, A' and B' in U_1, C' in U_2 and their diametrically opposite, i.e. A'', B'' and C'', in V_1 and V_2. A' and A'' are saddle-nodes, B' and B'' are repelling nodes, C' and C'' are attracting nodes. And systems (2) have only one finite equilibrium $(1, 0)$, which is a saddle. The saddle has four separatrices S_i $(i = 1, 2, 3, 4)$, S_1 connects $(1, 0)$ and the infinite equilibrium A'', S_2 connects $(1, 0)$ and the infinite equilibrium A', S_3 connects $(1, 0)$ and the infinite equilibrium C', and S_4 connects $(1, 0)$ and the infinite equilibrium C''. The saddle-node A' has the separatrix $S_5 = S_2$, and A'' has the separatrix $S_6 = S_1$, these separatrices are not at infinity.

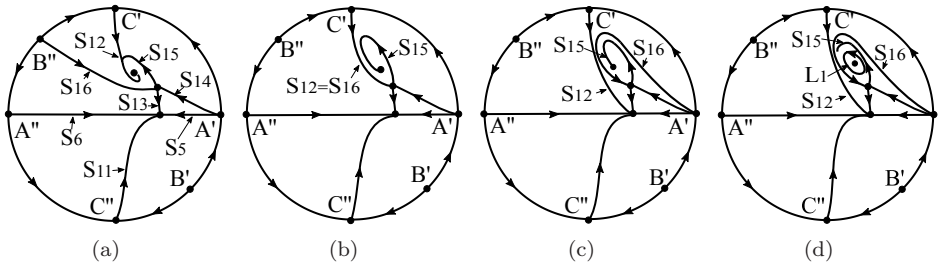

FIGURE 17. Some separatrices of the phase portraits. (a) phase portrait 1.5, (b) phase portrait 1.6, (c) phase portrait 1.7, (d) phase portrait 1.14.

On the bifurcation curve $a = f_1(b)$ with $b < 0$, we get the phase portrait 1.2, see Figure 16(b). This phase portrait has the finite equilibrium $(1/2, 1/(2b))$, which is a saddle-node. The saddle-node has three separatrices S_i $(i = 7, 8, 9)$, S_7 connects $(1/2, 1/(2b))$ and the infinite equilibrium C'', S_8 connects $(1/2, 1/(2b))$ and the infinite equilibrium A'', and S_9 connects $(1/2, 1/(2b))$ and the infinite equilibrium B'. The infinite equilibria keep their type.

When the parameter (a, b) in Figure 4 provides the phase portrait 1.3, see Figure 16(c), the saddle-node $(1/2, 1/(2b))$ of the phase portrait 1.2 splits into the attracting node $p_1 = (1/2 + \sqrt{a(a-4b^2)}/(2a), (a - \sqrt{a(a-4b^2)})/(2ab))$ and the saddle $p_2 = (1/2 - \sqrt{a(a-4b^2)}/(2a), (a + \sqrt{a(a-4b^2)})/(2ab))$. Then it generates the separatrix S_{10}, which connects p_1 and p_2.

On the bifurcation straight line $b = 0$ with $0 < a$ we have the phase portrait 1.4, see Figure 16(d). The node p_1 of the phase portrait 1.3 moves to $(1, 0)$, p_2 moves to the infinite equilibrium C'' in the local chart V_2, and the separatrices S_i $(i = 4, 7, 8, 9)$ disappear. C' and C'' become saddle-nodes. The saddle-node C' has one separatrix S_{11}, they are not at infinite. Hence systems (2) have only one finite equilibrium $(1, 0)$. This completes the description of the bifurcation diagram of Figure 4.

We start the analysis of the bifurcation diagram described in Figure 5. The phase portrait 1.4 has six infinite equilibria A', A'', B', B'', C' and C''. A', A'', C' and C'' are saddle-nodes, and B' and B'' are repelling nodes. There is only one finite equilibrium $(1, 0)$, which is a saddle-node. The saddle-node $(1, 0)$ has three separatrices S_i $(i = 1, 2, 3)$. A' has one separatrix $S_5 = S_2$, A'' has one separatrix $S_6 = S_1$, and C'' has one separatrix S_{11}, these separatrices are not at infinity.

When (a, b) in Figure 5 provides the phase portrait 1.5, see Figure 17(a), the finite saddle-node of the phase portrait 1.4 splits into two finite equilibria the same $(1, 0)$ (an attracting node) and the saddle p_1. The saddle-node C' splits into a saddle at C' and an attracting node or focus at p_2, which are connected by the separatrix S_{12}. The saddle p_1 has four separatrices S_i $(i = 13, 14, 15, 16)$, S_{13} connects p_1 and $(1, 0)$, S_{14} connects p_1 and the infinite equilibrium A', S_{15} connects p_1 and p_2, S_{16} connects p_1 and the infinite equilibrium B''. The saddle-node A' has one separatrix

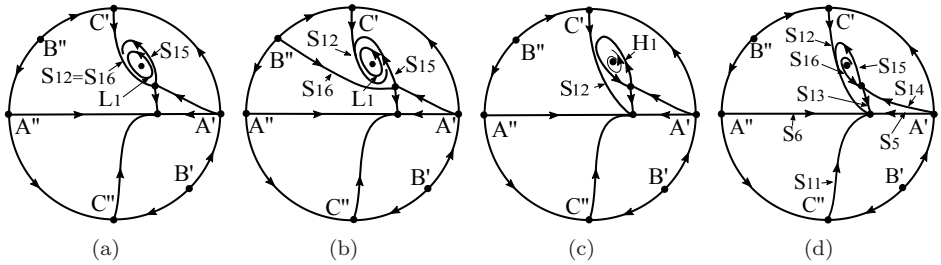

FIGURE 18. Some separatrices of the phase portraits. (a) phase portrait 1.15, (b) phase portrait 1.16, (c) phase portrait 1.13, (d) phase portrait 1.17.

S_5, A'' has one separatrix S_6, and the saddle C'' has one separatrix S_{11}, they are not at infinity.

As (a, b) reaches the bifurcation curve $a = f_5(b)$ we obtain the phase portrait 1.6, see Figure 17(b). The separatrix S_{16} of phase portrait 1.5, which connects the infinite equilibrium B'' with p_1, now it connects with the separatrix S_{12}.

When (a, b) in Figure 5 provides the phase portrait 1.7, see Figure 17(c), the separatrix S_{12} of phase portrait 1.6 goes to $(1, 0)$, and the separatrix S_{16} comes from A'.

When (a, b) provides the phase portrait 1.14, see Figure 17(d), the stability of the focus p_2 of the phase portrait 1.7 reverses, a Hopf bifurcation occurs, and a stable limit cycle L_1 bifurcates from p_2. Similarly we obtain the phase portraits 1.15 and 1.16 (see Figure 18(a) and 18(b)) from the phase portraits 1.6 and 1.5 , respectively.

When (a, b) is in the bifurcation curve $a = f_4(b)$ with $b \geq b_4$, we obtain the phase portrait 1.13, see Figure 18(c) (i.e. from the phase portrait 1.14 to the phase portrait 1.17). The limit cycle of the phase portrait 1.14 ends in the loop H_1 formed by the connection of the separatrices S_{15} and S_{16}.

When (a, b) provides the phase portrait 1.17, see Figure 18(d), the homoclinic loop H_1 of phase portrait 1.13 breaks up, and the separatrix S_{16} connects p_1 and p_2, and the separatrix S_{15} connects p_1 and $(1, 0)$.

When (a, b) is located in the bifurcation curve $a = f_1(b)$ with $b > 2$, see Figure 19(b), we obtain the phase portrait 1.22. The finite equilibria p_1 and p_2 of the phase portraits 1.17 collide providing a saddle-node, the separatrix S_{16} of the phase portrait of 1.17 disappears.

When (a, b) is the bifurcation point $(16, 2)$ we get the phase portrait 1.21, see Figure 19(a). The separatrix S_{15} of the phase portrait 1.22 connects with the separatrix S_{13}. Then the saddle-node p_1 becomes the cusp $(1/2, 1/4)$.

When (a, b) provides the phase portrait 1.23, see Figure 19(c), the finite singular point p_1 of the phase portrait 1.22 collides with $(1, 0)$, the separatrices $S_{13,14,15}$ disappear. Hence systems (2) have only one finite singular point which is an attracting node.

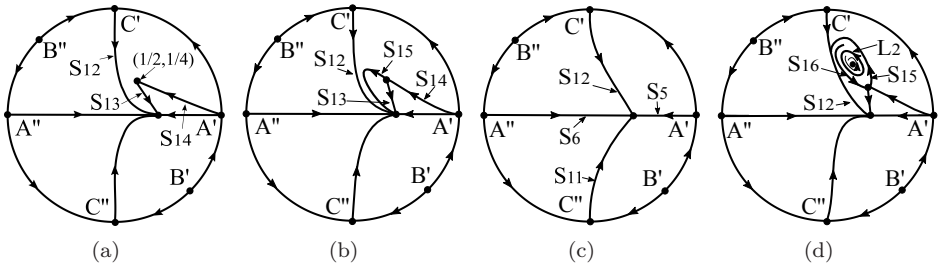

FIGURE 19. Some separatrices of the phase portraits. (a) phase portrait 1.21, (b) phase portrait 1.22, (c) phase portrait 1.23, (d) phase portrait 1.10.

When (a, b) provides the phase portrait 1.17 of Figure 5, systems (2) have six infinite equilibria A', A'', B', B'', C' and C''. A' and A'' are saddle-nodes, B' and B'' are repelling nodes, C' and C'' are saddles. A' has one separatrix S_5, A'' has one separatrix S_6, and C'' has one separatrix S_{11}, these separatrices are not at infinity. There are three finite equilibria $(1, 0)$ and $p_{1,2}$. $(1, 0)$ is an attracting node, p_1 is a saddle and p_2 is an unstable node or focus. p_1 has four separatrices $S_{13,14,15,16}$, and the separatrix S_{16} connects p_1 and p_2. When (a, b) is in the bifurcation curve $a = f_2(b)$ and $2 < b \leq 4$, the point p_2 becomes $p_2' = (1/b, (b-1)/b^2)$, and it is an unstable weak focus.

When (a, b) provides the phase portrait 1.10, see Figure 19(d), the stability of the focus p_2 of the phase portrait of 1.16 reverses, and an unstable limit cycle L_2 bifurcates from p_2'.

As (a, b) is in the bifurcation curve $a = f_4(b)$ with $2 < b < b_2$, we obtain the phase portrait 1.8, see Figure 20(a), the limit cycle of the phase portrait 1.9 ends in the homoclinic loop H_1 formed by the connection of sepeartrices S_{15} and S_{16}.

From the phase portrait 1.8 to 1.7, see Figure 17(c), the homoclinic loop H_1 of the phase portrait 1.8 breaks up, and the separatrix S_{15} connects the point p_1 and p_2, and the separatrix S_{16} connects the point p_1 and A'.

Now we consider the phase portraits 1.10 and 1.11. The stability of the focus p_2 of the phase portrait 1.10 reverses again, a Hopf bifurcation occurs, and a stable limit cycle L_1 bifurcates from this singular point. Hence there exist exactly two limit cycles in the phase portrait 1.11, one is stable and one is unstable, see Figure 20(c). Conversely the limit cycle L_1 of the phase portrait 1.11 becomes smaller and finally disappears .

When (a, b) is in the bifurcation curve $a = f_4(b)$ with $b_2 < b < b_4$, see Figure 20(b), we have the phase portrait 1.9. The bigger limit cycle L_2 of the phase portrait 1.11 ends in the homoclinic loop H_1 formed by the connection of separatrices $S_{15,16}$.

From the phase portrait 1.9 to 1.13, the limit cycle L_1 of the phase portrait 1.9 ends in the homoclinic loop H_1. From the phase portrait 1.8 to 1.9, the stability of the focus p_2 of the phase portrait 1.8 reverses, a Hopf bifurcation occurs, a stable

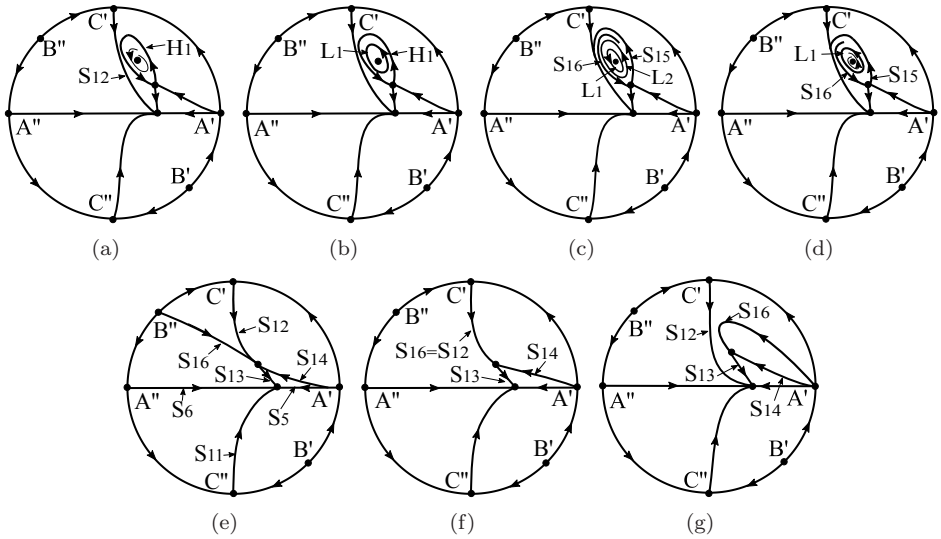

FIGURE 20. Some separatrices of the phase portraits. (a) phase portrait 1.8, (b) phase portrait 1.9, (c) phase portrait 1.11, (d) phase portrait 1.12, (e) phase portrait 1.18, (f) phase portrait 1.19, (g) phase portrait 1.20.

limit cycle L_1 bifurcates from p_2. Conversely the limit cycle L_1 of the phase portrait 1.9 becomes smaller and disappears.

When (a, b) is the bifurcation point $(f_4(b_2), b_2)$, see Figure 20(a), we obtain the phase portrait 1.8. The limit cycle L_1 of the phase portrait 1.10 becomes smaller and disappears in a Hopf bifurcation, and the limit cycle L_2 ends in the homoclinic loop H_1.

When (a, b) is in the bifurcation curve $a = f_3(b)$ with $4 < b < b_4$, the two limit cycles of the phase portrait 1.11 collide producing a semi-stable limit cycle in the phase portrait 1.12 (externally unstable and internally stable), see Figure 20(d). When the parameter (a, b) is the bifurcation point $(f_4(b_4), b_4)$ we obtain the phase portrait 1.13, see Figure 18(c). The semi-stable limit cycle of the phase portrait 1.12 ends the homoclinic loop H_1. When the parameter (a, b) produces the phase portrait 1.17, see Figure 18(d), the semi-stable limit cycle of the phase portrait 1.12 disappears.

On the other hand, when (a, b) provides the phase portrait 1.5, see Figure 17(a), systems (2) have six infinite equilibria A', A'', B', B'', C' and C''. A' and A'' are saddle-nodes, B' and B'' are repelling nodes, and C' and C'' are saddles. The saddle-node A' has one separatrix S_5, A'' has one separatrix S_6, the saddle C' has one separatrix S_{12} and C'' has one separatrix S_{11}, these separatrices are not at infinity. Systems (2) have three finite equilibria $(1, 0)$ and $p_{1,2}$. $(1, 0)$ is an attracting node, p_1 is a saddle and p_2 is an attracting node or focus. The saddle p_1 has four separatrices S_i $(i = 13, 14, 15, 16)$.

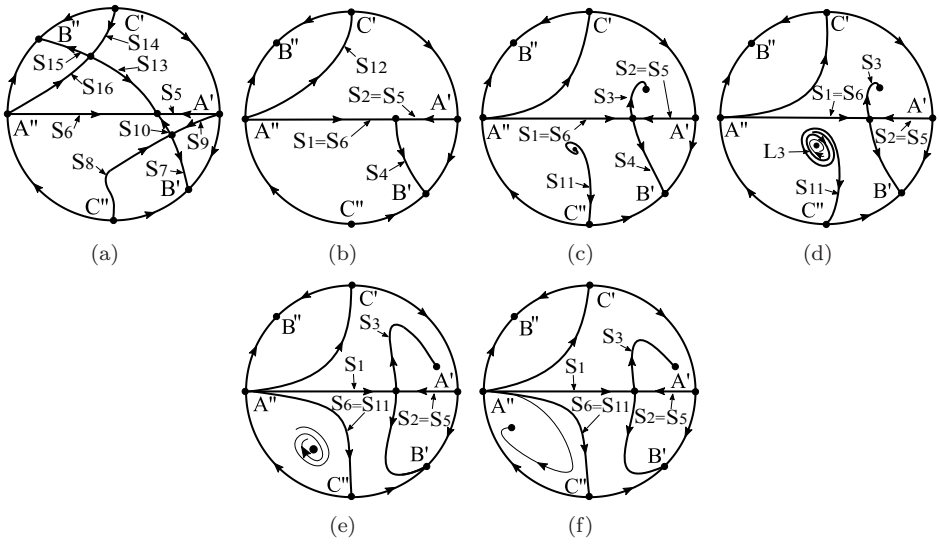

FIGURE 21. Some separatrices of the phase portraits. (a) phase portrait 1.24, (b) phase portrait 1.25, (c) phase portrait 1.26, (d) phase portrait 1.27, (e) phase portrait 1.28, (f) phase portrait 1.29.

When (a, b) is in the bifurcation curve $a = f_1(b)$ with $0 < b < b_1$, we get the phase portrait 1.18, see Figure 20(e). The finite equilibria p_1 and p_2 of the phase portraits 1.5 collide, and the separatrix S_{15} connecting them disappears.

When $(a, b) = (f_1(b_1), b_1)$, we have the phase portrait 1.19, see Figure 20(f). The separatrix S_{16} of the phase portrait 1.18 connects with the separatrix S_{12}.

When (a, b) is in the bifurcation curve $a = f_1(b)$ with $b_1 < b < 2$, we obtain the phase portrait 1.20, see Figure 20(g). The separatrix S_{16} of the phase portrait 1.19 connects with the infinite equilibrium A', and the separatrix S_{12} goes to $(1, 0)$.

When (a, b) reaches the bifurcation point $(16, 2)$ we get the phase portrait 1.21, see Figure 19(a). The separatrix S_{16} of the phase portrait 1.20 connects with the separatrix S_{14}. The saddle-node p_1 becomes now the cusp $(1/2, 1/4)$.

From the phase portrait 1.6 to the phase portrait 1.19, the finite singular point p_2 of the phase portrait 1.6 collides with p_1, and the separatrix S_{15} disappears. Then p_1 becomes a saddle-node. Similarly we obtain the phase portrait 1.20 from the phase portrait 1.7.

From the phase portrait 1.8 to the phase portrait 1.21, the finite singular point p_2 of the phase portrait 1.8 collides with p_1, and the homoclinic loop H_1 disappears. Then p_1 becomes a cusp.

Hence, we finish the analysis of the bifurcation diagram of Figure 5.

Next we summarize the change of the phase portraits from Figure 6. When the parameter (a, b) produces the phase portrait 1.24 , see Figure 21(a), systems (2)

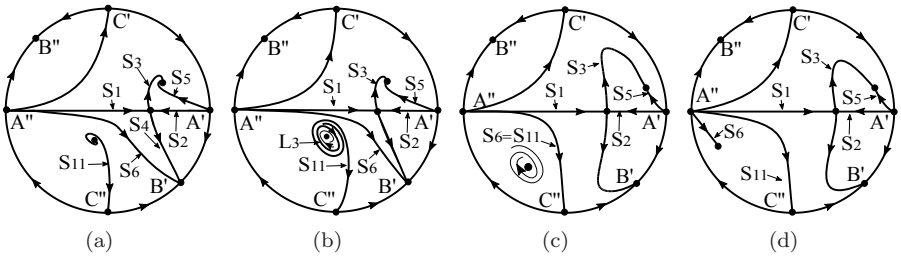

FIGURE 22. Some separatrices of the phase portraits. (a) phase portrait 1.30, (b) phase portrait 1.31, (c) phase portrait 1.32, (d) phase portrait 1.33.

have six infinite equilibria A', A'', B', B'', and C' and C''. A' and A'' are saddle-nodes, B' and B'' are attracting nodes, and C' and C'' are repelling nodes. The saddle-nodes A' and A'' have one separatrix S_5 and S_6 respectively, which are not at infinity. There are three finite singular points $(1,0)$ and $p_{1,2}$. $(1,0)$ is an attracting node and $p_{1,2}$ are saddles. p_1 and p_2 have four separatrices S_i $(i = 13, \cdots, 16)$ and four separatrices S_j $(j = 7, \cdots, 10)$, respectively.

On the bifurcation straight line $b = 0$ and $a < 0$, we obtain the phase portraits 1.25, see Figure 21(b). The point p_1 of the phase portrait 1.24 moves to the infinite point C' in U_2, p_2 moves to $(1,0)$, and the separatrices S_i $(i = 13, 14, 15, 17, 18, 19)$ disappear. The finite equilibrium $(1,0)$, the infinite equilibria C' and C'' become saddle-nodes. The saddle-node $(1,0)$ has three separatrices $S_{1,2,4}$, where $S_1 = S_6$ and $S_2 = S_5$. C' has one separatrix S_{12} which is not at infinity.

When the parameter (a,b) produces the phase portrait 1.26, see Figure 21(c). The saddle-node $(1,0)$ of the phase portrait 1.25 splits into an attracting node or a stable focus p_2 and a saddle $(1,0)$. The saddle $(1,0)$ has four separatrices $S_{1,2,3,4}$. The infinite saddle-node C'' splits into the same C'' (a saddle) and a repelling node or an unstable focus p_1. The saddle C'' has one separatrix S_{11} which is not at infinity. When (a,b) is in the bifurcation curve $a = f_2(b)$ and $-1 \le b < 0$, p_1 becomes an unstable weak focus $p_1' = (1/b, (b-1)/b^2)$.

When the parameter (a,b) produces the phase portrait 1.27, see Figure 21(d), the stability of the focus p_1' of the phase portrait 1.26 reverses, and a Hopf bifurcation occurs, and an unstable limit cycle L_3 bifurcates from p_1.

On the bifurcation curve $a = f_7(b)$ and $-1 \le b < 0$, we have the phase portrait 1.28, see Figure 21(e). The limit cycle L_3 and the separatrix $S_{6,11}$ of the phase portrait 1.27 collide, and connect with the infinity A'' producing a heteroclinic loop.

When the parameter (a,b) produces the phase portrait 1.29, see Figure 21(f), the orbit of the phase portrait 1.28 at p_1 connects with the infinite singular point A''.

When the parameter (a,b) produces the phase portrait 1.30, see Figure 22(a). The saddle $(1,0)$ has four separatrices $S_{1,2,3,4}$. The separatrix S_5 of the phase portrait 1.26 at the saddle-node A' moves to connect p_2, the separatrix S_6 at A''

moves to connect B'. Similarly we obtain the phase portrait 1.31 from the phase portrait 1.27, see Figure 22(b).

When the parameter (a, b) is in the bifurcation curve $a = f_7(b)$ and $b < -1$, we have the phase portrait 1.32, see Figure 22(c). The limit cycle L_3 and the separatrices $S_{6,11}$ of the phase portrait 1.31 collide, and it produces a heteroclinic loop.

When the parameter (a, b) produces the phase portrait 1.33, see Figure 22(d), the separatrix S_6 of the phase portrait 1.32 at the saddle-node A'' moves to connect with p_1. This completes the analysis of the bifurcation diagrams.

5. Conclusion

In this paper the phase portraits in the Poincaré disk for the cubic polynomial systems corresponding to the Gray-Scott model are studied in the Poincaré compactification. The phase portraits and the corresponding bifurcation diagrams show the richness and the complicated dynamics of such systems.

Acknowledgments

The first author is partially supported by National Natural Science Foundation of China (No. 11771059).

The second author is partially supported by the MINECO-FEDER grant MTM2016-77278-P, and the AGAUR grant 2017SGR-1617.

The third author is partially supported by the National Natural Science Foundations of China (No. 11401111,11661017), China Scholarship Council (No. 201608440447), Science and Technology Program of Guangzhou (No. 201707010426) and Natural Science Foundation of Guangdong Province (2017A030313010).

References

[1] M. J. Álvarez, A. Ferragut, and X. Jarque, "A survey on the blow up technique," Int. J. Bifurcation Chaos **31**, 3103–3118 (2011).
[2] J. Artés and J. Llibre, "Quadratic Hamiltonian vector fields," J. Differential Equations **107**, 80–95 (1994).
[3] I. Berenstein and Y. D. Decker, "Defect-mediated turbulence and transition to spatiotemporal intermittency in the Gray–Scott model," Chaos **24**, 043109 (2014).
[4] T. Blows and C. Rousseau, "Bifurcation at infinity in polynomial vector fields," J. Differential Equations **104**, 215–242 (1993).
[5] T. Chen, L. Huang, P. Yu, and W. Huang, "Bifurcation of limit cycles at infinity in piecewise polynomial systems," Nonlinear Anal. **41**, 82–106 (2018).
[6] I. Colak, J. Llibre, and C. Valls, "Hamiltonian linear type centers of linear plus cubic homogeneous polynomial vector fields," J. Differential Equations **257**, 1623–1661 (2014).
[7] I. Colak, J. Llibre, and C. Valls, "Hamiltonian nilpotent centers of linear plus cubic homogeneous polynomial vector fields," Adv. Math. **259**, 655–687 (2014).
[8] I. Colak, J. Llibre, and C. Valls, "Bifurcation diagrams for Hamiltonian linear type centers of linear plus cubic homogeneous polynomial vector fields," J. Differential Equations **258**, 846–879 (2015).
[9] I. Colak, J. Llibre, and C. Valls, "Bifurcation diagrams for Hamiltonian nilpotent centers of linear plus cubic homogeneous polynomial vector fields," J. Differential Equations **262**, 5518–5533 (2017).

[10] J. Delgado, L. I. Hernández-Martínez, and J. Pérez-López, "Global bifurcation map of the homogeneous states in the Gray-Scott model," Int. J. Bifurcation Chaos **27**, 1730024 (2017).
[11] F. Dumortier, J. Llibre, and J. Artés, *Qualitative Theory of Planar Differential Systems* (Universitext, Springer-Verlag, NewYork, 2006).
[12] A. Gasull, A. Guillamon, and V. Mañosa, "Phase portrait of Hamiltonian systems with homogeneous nonlinearities," Nonlinear Anal. **42**, 679–707 (2000).
[13] P. Gray and S. K. Scott, "Autocatalytic reactions in the isothermal, continuous stirred tank reactor: Isolas and other forms of multistability," Chemical Engineering Science **38**, 29–43 (1983).
[14] A. Guillamon and C. Pantazi, "Phase portraits of separable Hamiltonian systems," Nonlinear Anal. **74**, 4012–4035 (2011).
[15] Y. Martínez and C. Vidal, "Classification of global phase portraits and bifurcation diagrams of Hamiltonian systems with rational potential," J. Differential Equations **261**, 5923–5948 (2016).
[16] D. S. Morgan and T. J. Kaper, "Axisymmetric ring solutions of the 2D Gray–Scott model and their destabilization into spots," Physica D **192**, 33–62 (2004).
[17] D. Schlomiuk and N. Vulpe, "Global topological classification of Lotka-Volterra quadratic differential systems," Electronic J. Differential Equations **64**, 1–69 (2012).
[18] S. K. Scott, T. Boddington, and P. Gray, "Analytical expressions for effectiveness factors in non-isothermal spherical catalysts," Chemical Engineering Science **39**, 1087–1097 (1984).
[19] P. Yu and M. Han, "Twelve limit cycles in a cubic case of the 16th Hilbert problem," Int. J. Bifurcation Chaos **15**, 2191–2205 (2005).

[1] College of Mathematics and Econometrics, Hunan University, Changsha, 410082, PR China

E-mail address: chenting0715@126.com

[2] Departament de Matemàtiques, Universitat Autònoma de Barcelona, 08193 Bellaterra, Barcelona, Catalonia, Spain

E-mail address: jllibre@mat.uab.cat

[3] School of Statistics and Mathematics, Guangdong University of Finance and Economics, Guangzhou, 510320, PR China

E-mail address: lism1983@126.com